Manufacturing Rev. **7**, 20 (2020)
© S. Naik et al., Published by EDP Sciences 2020
https://doi.org/10.1051/mfreview/2020018

Manufacturing Review
Available online at:
https://mfr.edp-open.org

RESEARCH ARTICLE OPEN ACCESS

Analysis, predictive modelling and multi-response optimization in electrical discharge machining of Al-22%SiC metal matrix composite for minimization of surface roughness and hole overcut

Subhashree Naik, Sudhansu Ranjan Das*, and Debabrata Dhupal

Department of Production Engineering, Veer Surendra Sai University of Technology, Burla 768018, Odisha, India

Received: 27 March 2020 / Accepted: 23 May 2020

Abstract. Due to the widespread engineering applications of metal matrix composites especially in automotive, aerospace, military, and electricity industries; the achievement of desired shape and contour of the machined end product with intricate geometry and dimensions that are very challenging task. This experimental investigation deals with electrical discharge machining of newly engineered metal matrix composite of aluminum reinforced with 22 wt.% of silicon carbide particles (Al-22%SiC MMC) using a brass electrode to analyze the machined part quality concerning surface roughness and overcut. Forty-six sets of experimental trials are conducted by considering five machining parameters (discharge current, gap voltage, pulse-on-time, pulse-off-time and flushing pressure) based on Box-Behnken's design of experiments (BBDOEs). This article demonstrates the methodology for predictive modeling and multi-response optimization of machining accuracy and surface quality to enhance the hole quality in Al-SiC based MMC, employing response surface methodology (RSM) and desirability function approach (DFA). Finally, a novel approach has been proposed for economic analysis which estimated the total machining cost per part of rupees 211.08 during EDM of Al-SiC MMC under optimum machining conditions. Thereafter, under the influence of discharge current several observations are performed on machined surface morphology and hole characteristics by scanning electron microscope to establish the process. The result shows that discharge current has the significant contribution (38.16% for Ra, 37.12% in case of OC) in degradation of surface finish as well as the dimensional deviation of hole diameter, especially overcut. The machining data generated for the Al-SiC MMC will be useful for the industry.

Keywords: EDM / Al-SiC MMC / surface roughness / overcut / optimization / cost analysis

1 Introduction

With today's technologies, one of the important challenges for manufacturing industry is to provide workpieces with specified quality characteristics in the required quantity and in the fastest and most cost-effective way possible. Therefore, the improvement of the machining of newer materials and alloys becomes an absolute necessity in manufacturing process. Day-by-day, metal matrix composites (MMC) have increasingly widened their use in manufacturing sectors like aerospace, defense, manufacturing, automobile, electronic, and nuclear industries. These materials are extensively employed in different industrial applications to attain high performances due to their favorable characteristics such as lightweight, more excellent resistance to wear, high specific strength and high-temperature resistance than conventional materials [1]. Lightweight materials are mechanically consistent with lesser manufacturing costs. In the viewpoint of commercial production, the traditional machining techniques are incompetent to machine metal matrix composites for achieving the required accuracy as well as precision, intricate shapes, also time-consuming and sometimes not possible (i.e., extremely difficult to be machined). Such features on a component can be achieved only through the advanced manufacturing process. Recent past, electrical discharge machining (called, EDM) process have made an attention to be an effective technology for machining several hard and difficult-to-cut materials due to the intense heating generated along with localized electric spark that almost produces negligible cutting force including minimum stress on the machined surface for the removal of material, and high flexibility with versatility of production. Hence, the EDM process deals with as a

* e-mail: das.sudhansu83@gmail.com

This is an Open Access article distributed under the terms of the Creative Commons Attribution License (https://creativecommons.org/licenses/by/4.0), which permits unrestricted use, distribution, and reproduction in any medium, provided the original work is properly cited.

sustainable and reasonable unconventional process for MMCs.

However, due to the complex-dynamic behavior of EDM process and its close connection with various parameters, the achievement of high responsiveness of production is essential from the techno-economical point-of-views. Several factors influencing the cutting behaviour in EDM process are such as dielectric flushing pressure [2,3], electrode materials [4–8], electric spark variables (current, discharge voltage, frequency, pulse duration) [9–11], dielectric fluids [12–15], etc. Moreover, for successful implementation of EDM technology as the substitute of conventional machining of various difficult-to-cut materials can be improved in terms of cutting efficiency, quality, cost, and productivity by considering the most appropriate and optimal process parameters, which mainly consumes precious time and effort. Under such circumstances, the effective utilization of experimental, modeling, and optimization methodology make possible a more considerable improvement in decision-making with a new technological solution that can simultaneously satisfy and control the several distinctive as well as contradictory objectives (multi-objective) in order to make the EDM process an excellent choice for machining of advanced metal matrix composite materials. Several statistical and computational approaches such as RSM [16–21], ANN [22–27] have been applied for predictive modeling and Taguchi method [28–31], GRA [32–36], desirability function approach of RSM [37–40], and PCA [41,42] have been employed for parametric as well as process optimization in electrical discharge machining. Extensive studies have been reported by employing various experimental designs, modeling techniques and optimization approaches in order to assess or investigate the machinability [43–46], to predict the various technological responses, and to control the process parameters in machining of different workpiece materials (AISI D2, D3, D6, MDN 300, AISI 316L, stainless steel, A_2 tool steel, grey cast iron, Inconel 600, 601, 625, 825, 718, Ti6Al4V, Ti13Zr13Nb, nickel alloy, Al7075, Al6061, Al6063 alloy, Al-SiC MMC, Si_3N_4-TiN MMC, Al-Mg_2Si, WC, polycrystalline diamond). Table 1 overviews the extensive studies carried out to analyze, predict and control the machining performances in electrical discharge machining of various workpiece materials using different electrode materials under different machining conditions as well as various dielectric mediums.

On the basis of literature overview up to now, it is noticed that no credible studies were performed on machining of Al-22%SiC based MMCs by EDM process. Moreover, under high temperature and sharp cooling conditions, the melting metal particles re-solidify to form a thick recast layer on the surface of the hole. The blockage of the machining gap also leads to an increase in the concentration of contaminants in the working fluid. The poor decontamination of the working fluid may result in extra spark and secondary discharges, and these abnormal discharges cause instable machining, reducing the machining accuracy, surface quality, and machining efficiency. Moreover, because of the poor decontamination of the narrow gap and the high residual Joule heat, decreasing the quality of the machined surface. Hence, the removal of machining by-products is essential for achieving high machining accuracy and surface quality in EDM. Albeit many studies have been carried out in the past and reported in literatures on material removal rate, tool wear rate, and surface roughness as the center of attention towards assessing machining performance: aspects of machined surface morphology and machined hole characteristics have not been emphasized intensively. It was most solicited from an industrial standpoint to process in EDM with the possibility of achieving the good surface quality as well as hole quality. Though the implementation of RSM and desirability function approach was existent in the literatures, until now no systematic study has been reported to predict as well as to control surface quality and dimensional accuracy of the machined hole in the absence of MRR, EWR. Moreover, to the best of the author's knowledge, previous studies did not consider any economic analysis solution enabling cost-effective manufacturing using EDM, which finds the scope for researches from techno-economical point-of-view. In order to fill up the existing research gap, the process work addresses the workpiece surface finish and hole overcut during electrical discharge machining of newly engineered metal matrix composite (MMC) of aluminum reinforced with 22 wt.% of SiC particles with brass electrode. A methodology for predictive modelling and multi-response optimization has been developed by employing response surface methodology (RSM) and desirability function approach (DFA). Additionally, an out of the paradigm investigation of EDM on Al-SiC MMC has been made to analyze how the discharge current affects the hole quality as well as surface finish of the machined component. Finally, a unique economic analysis has been performed: (i) to rationalize the usefulness of EDM process for difficult as well as hard-to-cut materials, and (ii) to confirm the feasibility of the EDM strategy for mass production in industry. Hence, the gap between the literature and the current research is somewhat diminished. Novelty aspect, the present study will be useful as technological guidelines for practical industrial application of EDM process in automotive, aerospace, military, and electricity industries to establish a superior advantage of mechanism from the economical point of view. All of these points bring worthy investigations, contribute to the uniqueness of the current study, and make advancements towards economic manufacturing.

2 Experimental setup and procedure

In this work, conductive silicon carbide particle reinforced aluminum-based metal matrix composite (Al-SiC MMC) of a circular plate having dimensions ϕ65 mm × 5 mm (diameter and thickness, respectively) is selected as workpiece material because of its excellent-unique characteristics (lightweight, strength, hardness, stiffness, wear, and corrosion resistance) as well as due to its economic production and its widespread application in aerospace, automobiles industries. For the preparation of workpiece material, the furnace was preheated at a temperature of 400 °C. Scraps of aluminum of around 1 kg were preheated

Table 1. Literature overview.

References	Workpiece materials	Electrode materials	Dielectric medium	Process parameters	Machining characteristics	Techniques	Research findings
[1]	Al–SiC metal matrix composite	Brass	Kerosene	Discharge current, pulse duration, speed of electrode rotation, hole diameter of the electrode, polarity of the electrode, volume percentage of SiC	Material removal rate, electrode wear rate, surface roughness	GA	• With the increase in volume percentage of SiC, MRR decreases and EWR increases. • With the decrease in hole diameter and increase in speed of the rotating tube electrode, MRR increases and EWR and SR decreases.
[2]	WC/30%Co composite	Copper	Kerosene	Electrode rotation, pulse on time, current, flushing pressure	Material removal rate, surface roughness	RSM	• Combination of low pulse time and high peak current, rotational speed, and flushing pressure yields more MRR and less Ra. • Surface finish improves at higher levels of electrode rotation and flushing pressure
[3]	Titanium alloy (Ti-6Al-4V)	Copper	EDM oil	Pulse-on time, peak current, gap voltage, spindle speed, flushing pressure	Material removal rate, surface roughness	Taguchi method	• Peak current has the most significant effect on MRR, whereas the pulse-on time and gap voltage show almost the same effect, over MRR • Surface roughness is affected by peak current and pulse-on time while gap voltage and spindle speed have no effect.
[4]	AISI D3 tool steel	Copper	Kerosene	Pulse current, pulse-on time, pulse-off time, gap voltage	Overcut	RSM	• Overcut is significantly affected by pulse-on time and pulse current but pulse-off time and gap voltage have less effect.
[5]	Inconel 718	Brass		Discharge current, open-circuit voltage, pulse-on time, duty factor, flushing pressure, cryogenic treatment soaking duration of brass tool	Electrode wear ratio, surface roughness, radial overcut	TOPSIS, TLBO	• Deep cryogenic treated brass tool with longer soaking duration has been proven to be an ideal EDM tool to machine hard materials like Inconel 718.

Table 1. (continued).

References	Workpiece materials	Electrode materials	Dielectric medium	Process parameters	Machining characteristics	Techniques	Research findings
[6]	Inconel 718	Copper, graphite, brass	Paraffin oil	Open circuit voltage, discharge current, pulse-on-time, duty factor, flushing pressure, electrode material	Material removal rate, tool wear rate, surface roughness, radial overcut	PSO	• Material removal rate can be maximized with the use of graphite tool and minimized using brass electrode but better surface integrity can be obtained using brass electrode. • Tool wear decreases using graphite tool compared to copper and brass tool. • QPSO provides better result than PSO resulting.
[7]	Tungsten carbide	Copper, tungsten	EDM 22 mineral oil	Electrode material, polarity, open-circuit voltage, peak current, pulse duration, pulse interval, flushing pressure	Material removal rate, relative wear ratio, surface roughness		• Material removal rate and the surface roughness are directly proportional to the peak current.
[8]	Titanium Grade 6 alloy (Ti-5Al-2.5Sn)	Copper, brass, zinc		Pulse on time, peak current, gap voltage. Duty cycle	Material removal rate, tool wear rate	RSM	• Material removal rate can be maximized with the use of brass and zinc electrodes compared to copper electrode. • Tool wear and recast layer can be reduced with the use of brass and zinc electrodes.
[9]	Titanium alloy (Ti-6Al-4V)	Tungsten, copper, cryogenically treated copper	EDM 30 oil	Peak discharge current, pulse-on time, gap voltage, duty factor, dielectric flushing pressure, spark gap, machining time	Material removal efficiency, surface roughness, surface crack density, white layer thickness		• Cryogenically treated Copper has exhibited higher micro-hardness value, higher MRR, improved surface finish and lower tool wear as compared to normal Copper. • Lower MRR and too rough surface has obtained by using tungsten electrode.
[10]	Al6061-SiC MMC	Copper, brass, stainless steel	Kerosene oil mixed with grapheme nanoparticle	Current intensity, pulse duration, duty cycle	Material removal rate, surface roughness, electrode wear ratio	RSM	• Brass electrode yielded higher MRR and better surface finish than copper and stainless steel electrodes.

Table 1. (continued).

References	Workpiece materials	Electrode materials	Dielectric medium	Process parameters	Machining characteristics	Techniques	Research findings
							• Lower EWR resulted by using stainless steel electrode than copper and brass electrodes.
[11]	Inconel 825	Graphite, tungsten, brass, copper	EDM 30 oil	Peak discharge current, gap voltage, pulse-on time, duty factor, flushing pressure	Material removal rate, surface roughness, surface crack density, white layer thickness		• Copper electrode yielded higher MRR. • Increase in peak discharge current, increases the material removal rate, surface roughness, white layer thickness etc.
[12]	Titanium alloy (Ti-6Al-4V)	Cu-TaC composite	Urea solution, distilled water	Peak current, pulse duration	Surface roughness, microhardness		• Distilled water dielectric fluid gave better surface roughness, while use of urea solution gives higher surface roughness.
[13]	AISI 8407 steel	Steel needle	Oxygen, air, kerosene, deionized water, water-in-oil emulsion	Pulse duration, type of dielectrics	Hole geometry, craters, recast layer thickness, material removal rate		• Different shape of craters formed in different dielectrics with the same experimental conditions • Higher removal has been obtained in liquid dielectrics compared to gaseous dielectrics • Kerosene resulted in higher removal efficiency; less volume of material was melted compared to other dielectrics.
[14]	Aluminium alloy 6063	Copper	Biodiesel, transformer oil, kerosene	Peak current, pulse on time, pulse off time, different dielectrics	Material removal rate, electrode Wear, surface roughness	Taguchi method	• biodiesel gives high MRR and less EWR compared to kerosene dielectric • The material removal rate and electrode wear rate are mainly affected by peak current followed by the pulse on time with negligible effect of pulse off time.

Table 1. (continued).

References	Workpiece materials	Electrode materials	Dielectric medium	Process parameters	Machining characteristics	Techniques	Research findings
[15]	Inconel 738	Brass	Kerosene, deionized, water, EDM emulsion, water solution EDM fluid	Open circuit voltage, current peak, pulse duration, pulse interval	Material removal rate, electrode wear, holes generation, recast layer formation	Taguchi method	• The recast layer became thicker with the increase in electric conductivity of dielectric fluids. • The recast layer became thin with kerosene but due to decomposition of kerosene, the machining speed was low.
[16]	Spheroidal graphite cast iron	Copper	Kerosene	Diameter of graphite particle, quantity of graphite particle, area fraction of graphite particle	Layer thickness, Ridge density	RSM	• Layer thickness increases with the increase of the quantity and area fraction of graphite particle but it reduces with the increase of diameter of graphite particle.
[17]	Al/SiC metal matrix composite	Copper	Kerosene	Pulse on time, peak current, average gap voltage, volume fraction of SiC in aluminium matrix	Material removal rate, electrode wear ratio, gap size, surface finish	RSM	• MRR becomes higher with an increase of pulse on time, peak current and relatively with gap voltage and reduces with increase of SiC percentage. • EWR becomes higher with an increase of both pulse on time and peak current and reduces with increase of both of SiC percentage and gap voltage. • Surface roughness increases with the increase of pulse on time, SiC percentage, peak current, gap voltage.
[18]	AISI D2 tool steel	Graphite	Kerosene mixed with carbon nanotube	Discharge current, discharge duration, discharge voltage	Surface roughness, morphology, micro-cracks	RSM, fuzzy logic modelling	• Micro-cracks with CNT are less than that without CNTs. • The maximum test errors for surface roughness and micro-cracks using response surface model are more without CNTs compared to with CNTs.

Table 1. (continued).

References	Workpiece materials	Electrode materials	Dielectric medium	Process parameters	Machining characteristics	Techniques	Research findings
[19]	Al-Mg_2Si metal matrix composite	Copper	Dielectric fluid mixed with aluminium powder	Voltage, current, pulse on time, duty factor	Material removal rate, electrode wear ratio, microstructure changes	RSM	• MRR is significantly affected by voltage, current and EWR is significantly affected by pulses ON time. • It was obtained from the microstructure analysis that voltage, current, and pulse ON time have a significant effect on machined surface profile.
[20]	AISI D6 tool steel	Copper	Kerosene	Pulse on time, pulse current, voltage	Material removal rate, tool wear ratio	RSM	• Increased pulse on time resulted in higher material removal rate and reduced tool wear ratio. • Both material removal rate and tool wear ratio become maximum by increasing the pulse current and reduces at higher value of the input voltage respectively.
[21]	Titanium Ti-13Nb-13Zr alloy	Graphite	Kerosene	Current, voltage, pulse on time, pulse off time	Material removal rate, electrode wear rate, surface roughness	RSM	• The absolute error between predictions and actual values fall within 10% for which the model can be effectively used to predict the EDM machining parameters.
[24]	AISI D2 steel	Copper	EDM oil	Pulse current, pulse on time, duty cycle	Surface roughness	ANN	• The process performance with accuracy could be predicted using neural models under different machining conditions. • RBFN is faster than the BPNs and the BPN is reasonably more accurate.

Table 1. (continued).

References	Workpiece materials	Electrode materials	Dielectric medium	Process parameters	Machining characteristics	Techniques	Research findings
[25]	Al/SiC MMC	Copper, graphite, copper–graphite composite	EDM oil, EDM oil + copper powder, EDM oil + graphite powder	Workpiece, electrode, current, pulse-on time, pulse-off time, dielectric fluid	Residual stress	ANN	• MMCs with low coefficient of thermal expansion and a high density of reinforced particle have lower residual stresses. • The residual stresses reduced by adding powder in the dielectric.
[26]	Titanium alloy	Copper, copper-chromium, copper-tungsten	Ferrolac 3M EDM oil	Peak current, pulse-on-time, pulse-off-time, dielectric fluid mixed with powder, electrode material, cryogenic of electrode material, workpiece material, cryogenic workpiece material	Surface roughness	Hybrid Taguchi-ANN approach	• High discharge energy resulted as surface defects such as cracks, craters, thick recast layer, micro pores, pin holes, residual stresses and debris.
[27]	Polycrystalline diamond	Copper-tungsten, copper-nickel	Kerosene	Peak current, pulse interval, pulse duration	Material removal rate, electrode wear rate	ANN	• Copper tungsten electrode gave lower EWR, in comparison with the copper nickel electrode.
[28]	Inconel 718	Tungsten carbide	Kerosene	Peak current, pulse on-time, pulse off-time, spark gap	Electrode wear, material removal rate, working gap	Grey-Taguchi method	• Grey-Taguchi method is very suitable for solving the quality problem of machining in the micro milling EDM of Inconel 718
[29]	Maraging steel (MDN 300)	Copper		Discharge current, pulse on time, pulse off time	Material removal rate, tool wear rate, relative wear ratio, surface roughness	Taguchi method	• Discharge current is more significant than pulse on time for MRR and TWR. • Higher discharge current and longer pulse on duration gives rougher surface with more craters, globules of debris, and microcracks.
[30]	S-03 special stainless steel	Copper	Kerosene	Gap voltage, peak discharge current, pulse width, pulse interval	Material removal rate, surface roughness	Taguchi method, grey relational analysis	• The EDM high-accuracy process parameters sequenced in order of: peak discharge current, pulse interval, gap voltage, and pulse width. • The machined work piece has no surface modification layer.

Table 1. (continued).

References	Workpiece materials	Electrode materials	Dielectric medium	Process parameters	Machining characteristics	Techniques	Research findings
[31]	NiTi alloys	Copper		Gap current, pulse on time, pulse off time, workpiece electrical conductivity, tool conductivity	Material removal rate	Taguchi method	• The material removal rate affected by the significant the material removal rate parameters like work electrical conductivity, gap current and pulse on time.
[32]	SS 304	WC	Kerosene	Voltage, capacitance, resistance, feed rate, spindle speed	Electrode wear, entrance clearance, exit clearance, machining time, number of shorts	Taguchi method, grey relational analysis	• Electrode wear and the entrance and exit clearances have a significant effect on the diameter of the micro-hole when the diameter of the electrode is identical.
[33]	6061Al/Al_2O_3p/20P aluminium MMC	Copper		Pulse current, pulse ON time, duty cycle, gap voltage, tool electrode lift time	Material removal rate, tool wear rate, surface roughness	Grey relational analysis	• The sequence of the process parameters to the multi-performance characteristics is in the order of: pulse current, aspect ratio, tool electrode lift time, pulse ON time, gap voltage and duty cycle. • Grey system theory is designed to work with system where the available information is not sufficient to characterise the system.
[34]	Nickel-based superalloy	Copper		Gap voltage, gap current, pulse on time, duty factor, polarity, tool & workpiece materials, type of dielectrics, flow rate, flushing pressure, rotation of electrode or workpiece	Material removal rate, surface roughness, circularity	Taguchi method, RSM, PCA-GRA	• MRR become improves with the use of present hybrid approach in this experimental study.
[35]	Al7075	Brass	Deionized water	Pulse on-time, pulse off-time, flushing pressure	Material removal rate, tool wear rate	Grey relational analysis	• The optimization results showed that the MRR become maximum due to combination of higher pulse on-time and reduced pulse off-time.

Table 1. (continued).

References	Workpiece materials	Electrode materials	Dielectric medium	Process parameters	Machining characteristics	Techniques	Research findings
							• Tool wear rate was highly affected by pulse on-time, pulse off-time.
[36]	Si_3N_4-TiN composites	Copper		Current, pulse on time, pulse off time, dielectric pressure, gap voltage	MRR, electrode wear rate, surface roughness, radial overcut, taper angle, circularity, cylindricity, perpendicularity	GRA-RSM	• MRR increases with increase in discharge current and pulse on time. • EWR increases with increase in discharge current and pulse on time, and decrease in gap voltage. • The surface roughness decreases with decrease in discharge current whereas increasing gap voltage reduces surface roughness.
[37]	JIS SKD 61 alloy tool steel	Copper		Discharge current, gap voltage, pulse on-time, pulse off-time	Material removal rate, relative electrode wear ratio, surface finish	RSM, GA	• MRR increases due to a more powerful spark energy, at higher discharge current and pulse on time. • Larger thickness of recast layer was formed on the machined surface due to the powerful spark energy. • Relative electrode wear ratio reduces with increase of pulse on-time.
[38]	Al–SiC nano-composites	Copper		Voltage, pulse current, pulse on time, pulse off time	Material removal rate, electrode wear rate, surface roughness	RSM	• MRR increases with an increase in pulse on time and then with further increase in pulse on time. • MRR and surface roughness is mainly affected by pulse current and pulse on time.

Table 1. (continued).

References	Workpiece materials	Electrode materials	Dielectric medium	Process parameters	Machining characteristics	Techniques	Research findings
[39]	Aluminium-multiwall carbon Nano- tube composites (AL-CNT)	Copper	Kerosene	Machining-on time, discharge current, voltage, total depth of cut	Material removal rate, wear electrode ratio, surface roughness	Taguchi method, RSM	• As the number of trials increases over wider domains of process variables, the accuracy of these models is enhanced. • This methodology gathers experimental results, builds mathematical models in the domain of interest and optimizes the process models.
[40]	Tool steel 55NiCrMoV7	Graphite (EDM-3 POCO)	EDM fluid 108 MP-SE 60		Material removal rate	RSM	• Increase in the discharge current and pulse time leads to generation of craters with a larger depth and diameter. • Inter pulse time did not affect the change in surface integrity and the MRR significantly.
[42]	A2 tool steel	Copper	EDM-30	Discharge current, pulse on time, duty cycle, discharge voltage	Material removal rate, Electrode wear rate	Principal component analysis	• Discharge current is directly proportional to both MRR and EWR • Discharge current is having the maximum contribution towards MRR, while pulse on time is having maximum contribution towards EWR
[43]	Beryllium–copper alloy	C-122 copper	EDM-244 oil, deionized water	Dielectric medium, pulse on/off time, working current	material removal rate, electrode wear ratio, surface roughness	Taguchi method, GRA, RSM	• MRR is mostly affected by the working current, while the dielectric medium is the dominant parameter for EWR and Ra.
[44]	AISI 202 steel	Tungsten carbide	Kerosene	Discharge current, gap voltage, duty factor	Material removal rate, surface roughness	Taguchi method	• Better surface finish with high MRR could be produced by the modified ISO current pulse generator.

Table 1. (continued).

References	Workpiece materials	Electrode materials	Dielectric medium	Process parameters	Machining characteristics	Techniques	Research findings
[45]	Inconel 600	Graphite	Mineral oil	Current intensity, pulse time, duty cycle, open-circuit voltage, flushing pressure	Material removal rate, electrode wear, surface roughness	RSM	• Positive polarity results in higher MRR. • Both the production costs and production time decreases with an increase in current intensity.
[46]	Inconel 601, 625, 718, 825 super alloys	Graphite	EDM oil	Gap voltage, peak discharge current, pulse-on time, duty factor, flushing pressure	Material removal rate, electrode wear rate; surface roughness, surface crack density	Satisfaction function approach integrated with Taguchi method	• MRR and surface roughness increases with peak current.

at 450 °C for 2–3 h, and 3–4 pouches of silicon carbide (having a mesh size of about 300–400 microns) powder of 10 grams each were taken and melted along with the aluminum scraps at a temperature of 800 °C in a crucible. A higher amount of aluminum and silicon carbide was added to the crucible in order to prevent material loss. The molten material was stirred vigorously and was immediately cast into a graphite mold to obtain a tapered-cylindrical ingot of around 70 mm diameter. The diffusion of aluminum silicon carbide occurs in three stages; aluminum-aluminum (Al-Al), aluminum-silicon carbide (Al-SiC), silicon carbide-silicon carbide (SiC-SiC). The grain growth rate of SiC-SiC is much faster than the other two combinations, which, if not controlled might dominate the final grain structure of the material. In order to not let this happen, a small amount of around 0.1% NaCl powder was added just before casting. A tapered cylindrical piece of Al-SiC (22.13% SiC) of fine grain structure was thus obtained. For the present experimental purpose, the ingot was cut by a wire-EDM into six pieces with the piece having an average diameter of 65 mm, and each piece having a thickness of 5 mm. The elemental constituents and particle shape characterization of Al-SiC MMC are identified (refer, Fig. 1) in a scanning electron microscope (SEM) with an embedded energy dispersive X-ray (EDS) analyzer. Commercially available brass rod with diameter of 9 mm has been considered for electrode material in machining. Bio-degradable vegetable oil (with density: 0.917 g/cm^3; dynamic viscosity 48.4 g/m-s; dielectric rigidity: 62 kV/mm; specific heat: 1.67 J/g-K) was employed as dielectric medium.

For performing a series of experiments, a high accuracy computer numerical controlled electrical discharge machine tool (make: ECOWIN, model: MIC 432CS) has been utilized with maximum working current of 60 amp manufactured by Taiwan. During electrical discharge machining of Al-SiC MMC, the measurement of surface finish of machined hole part in term of arithmetical average roughness (Ra) is measured by Surftest SJ-210 Mitutoyo roughness tester. After every successive experimental trial, the overcut (OC) of the machined hole on Al-SiC MMC material is evaluated by employing co-ordinate measuring machine (ZEISS MC850), equipped with a stylus probe accessory. For better understanding of electrical discharge machining process as well as for machinability improvement, a comprehensive investigation is performed on the morphological study of machined surface by employing scanning electron microscope (JEOL JSM-6480LV). A scheme of the experimental setup with methodologies proposed in this work, is pictorially presented in Figure 2.

In this experimental investigation, five machining parameters (discharge current, gap voltage, pulse-on-time, pulse-off-time, flushing pressure) and two major technological performance characteristics (surface roughness, and overcut) of machined part are considered as input process factors and output responses, respectively. The selection of different levels of machining parameters are considered with reference to published research work [37,46] and by inspecting the workpiece for a through-hole of acceptable quality. Moreover, preliminary trails were executed to choose the appropriate range of each input parameters.

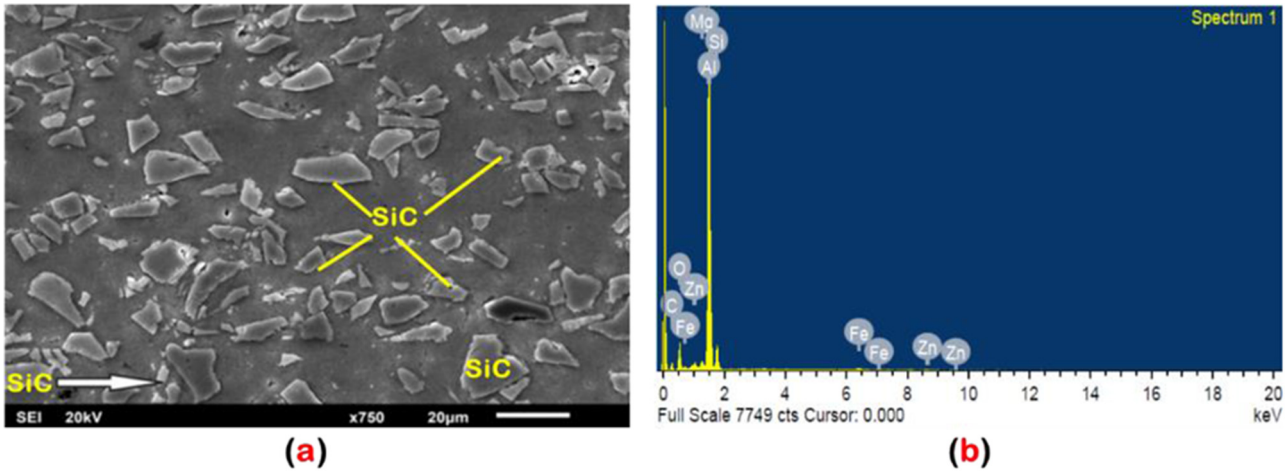

Fig. 1. Microstructure of Al-22%SiC MMC: (a) SEM micrograph and (b) EDX analysis.

Table 2. Machining process parameters associated with their coded value of levels.

Process parameters	Coded levels		
	−1	0	1
Discharge current, DC (amp)	5	10	15
Gap voltage, GV (V)	1	1.5	2
Pulse-on-time, TON (μs)	100	200	300
Pulse-off-time, TOFF (μs)	10	20	30
Flushing pressure, FP (kgf/cm^2)	0.2	0.4	0.6

Table 2 illustrates the detailed input factors with their corresponding levels for the experiment in actual as well as coded values setting. The proposed experimental design involves the variation of five factors (DC, GV, TON, TOFF, FP) at three levels. Machining trials are completely conducted based on Box-Behnken design of experiments associated with forty-six numbers of trial runs. The experimental design layout and results of machining trials are reported in Table 3.

3 Results and discussion

3.1 Development of predictive model using response surface methodology

In the present work, Design expert 11.0 is employed to analyze the obtained experimental results of the technological responses of machined part quality (here, surface roughness and overcut) in accordance with Box-Behnken DOEs through RSM. It is used to develop a best fitted empirical model that establishes a correlation between the machining response characteristics (surface finish of the machined component Ra, and overcut of drilled hole OC) with the given machining process parameters (DC, GV, TON, TOFF, FP). Regression equations for each response are presented by,

$$\begin{aligned}\text{Ra} = {} & 1.032 + 0.0548\text{DC} + 0.725\text{GV} - 0.00254\text{TON} - 0.0624\text{TOFF} - 3.996\text{FP} - 0.002427\text{DC}^2 - 0.1621\text{GV}^2 + 0.000001\text{TON}^2 + 0.000249\text{TOFF}^2 + 1.875\text{FP}^2 - 0.0374\text{DC*GV} - 0.000108\text{DC}*\text{TON} + 0.002565\text{DC}*\text{TOFF} + 0.1312\text{DC*FP} - 0.000180\text{GV*TON} + 0.00430\text{GV*TOFF} + 0.022\text{GV*FP} + 0.000087\text{TON*TOFF} + 0.0051\text{TON*FP} + 0.0221\text{TOFF*FP}\end{aligned}$$

$$R^2 = 88.92\%,\ R^2(\text{adj.}) = 80.05\% \quad (1)$$

$$\begin{aligned}\text{OC} = {} & 0.020 + 0.01255\text{DC} - 0.0877\text{GV} + 0.001718\text{TON} + 0.01002\text{TOFF} + 0.001\text{FP} + 0.001055\text{DC}^2 + 0.0393\text{GV}^2 - 0.000001\text{TON}^2 - 0.000159\text{TOFF}^2 - 0.272\text{FP}^2 - 0.01407\text{DC}*\text{GV} - 0.000069\text{DC}*\text{TON} + 0.000286\text{DC*TOFF} + 0.01258\text{DC*FP} + 0.000010\text{GV*TON} + 0.00197\text{GV*TOFF} + 0.0850\text{GV*FP} - 0.000033\text{TON*TOFF} + 0.000548\text{TON*FP} - 0.00841\text{TOFF*FP}\end{aligned}$$

$$R^2 = 93.69\%,\ R^2(\text{adj.}) = 88.64\% \quad (2)$$

The results obtained for the surface roughness (Ra) and overcut (OC) from machining experiment were analysed by employing ANOVA. Analysis of variance is a statistical tool, used to illustrate the validation of obtained experimental result. It is also applied to determine the significant effect of selected machining parameters and their interaction effect upon corresponding output responses. The ANOVA table consists of degree of freedom (DoF), sum and mean of squares (SS and MS), factor contribution in total variation (Contr. %), probability (P) and F-value. The statistical tools namely P-value and F-value are employed to determine the statistical significance and adequacy of developed regression model. If the P-value for any input parameter found to be under 0.05 (i.e. for 95% confidence level), then that input parameter may be considered as having statistically significant influence on corresponding output which is desirable [47]. If the calculated F-value is lower than the standardized Fisher's value or P-value is greater than 0.05 for any factor, then that parameter considered as no effect on output. From Table 4a, it is observed that the developed model for

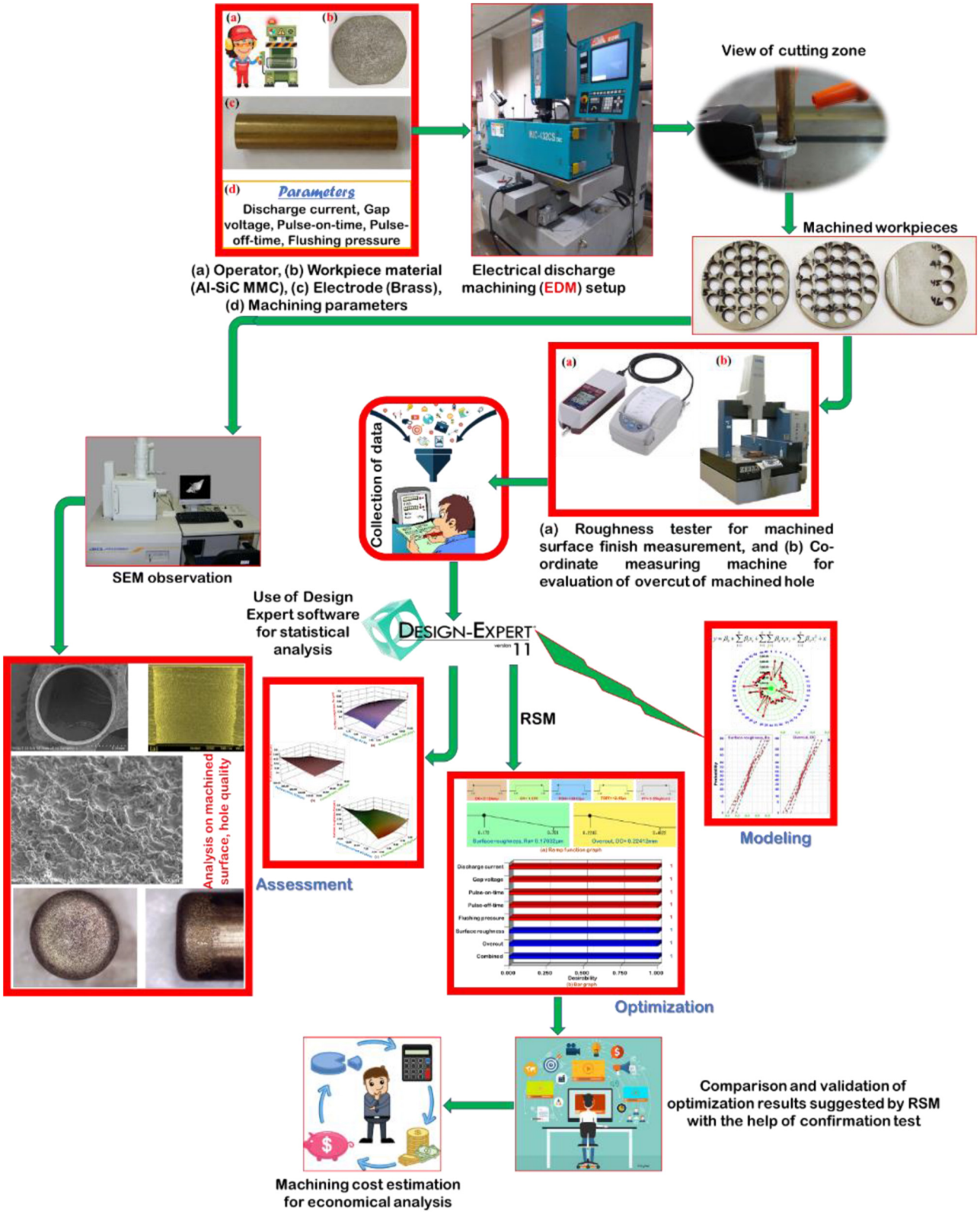

Fig. 2. Schematic of experimental setup with methodologies proposed.

surface roughness in electric discharge machining is significant as its *P*-value is desirable (i.e., under 0.05). After the execution of the analysis, it is also observed that DC, GV, TOFF, FP, DC*DC, FP*FP, DC*GV, DC*TOFF, DC*FP, TON*TOFF and TON*FP are the significant terms affecting Ra. However, among all the significant process parameters, the discharge current with 38.16% contribution has the most significant effect on

Table 3. Experimental plan layout and results.

	Coded values					Actual settings					Technological parameters	
Test. no.	DC	GV	TON	TOFF	FP	DC (amp)	GV (V)	TON (μs)	TOFF (μs)	FP (kgf/cm^2)	Ra (μm)	OC (mm)
1	−1	−1	0	0	0	5	1.0	200	20	0.4	0.177	0.3194
2	1	−1	0	0	0	15	1.0	200	20	0.4	0.7	0.4622
3	−1	1	0	0	0	5	2.0	200	20	0.4	0.205	0.345
4	1	1	0	0	0	15	2.0	200	20	0.4	0.354	0.3471
5	0	0	−1	−1	0	10	1.5	100	10	0.4	0.419	0.251
6	0	0	1	−1	0	10	1.5	300	10	0.4	0.389	0.3821
7	0	0	−1	1	0	10	1.5	100	30	0.4	0.4	0.3174
8	0	0	1	1	0	10	1.5	300	30	0.4	0.718	0.3148
9	0	−1	0	0	−1	10	1.0	200	20	0.2	0.455	0.3672
10	0	1	0	0	−1	10	2.0	200	20	0.2	0.404	0.2924
11	0	−1	0	0	1	10	1.0	200	20	0.6	0.463	0.3532
12	0	1	0	0	1	10	2.0	200	20	0.6	0.421	0.3124
13	−1	0	−1	0	0	5	1.5	100	20	0.4	0.187	0.2245
14	1	0	−1	0	0	15	1.5	100	20	0.4	0.6242	0.4118
15	−1	0	1	0	0	5	1.5	300	20	0.4	0.211	0.3608
16	1	0	1	0	0	15	1.5	300	20	0.4	0.433	0.4099
17	0	0	0	−1	−1	10	1.5	200	10	0.2	0.414	0.3003
18	0	0	0	1	−1	10	1.5	200	30	0.2	0.428	0.3166
19	0	0	0	−1	1	10	1.5	200	10	0.6	0.5685	0.3138
20	0	0	0	1	1	10	1.5	200	30	0.6	0.759	0.2628
21	0	−1	−1	0	0	10	1.0	100	20	0.4	0.381	0.3075
22	0	1	−1	0	0	10	2.0	100	20	0.4	0.345	0.2904
23	0	−1	1	0	0	10	1.0	300	20	0.4	0.458	0.3698
24	0	1	1	0	0	10	2.0	300	20	0.4	0.386	0.3548
25	−1	0	0	−1	0	5	1.5	200	10	0.4	0.221	0.3152
26	1	0	0	−1	0	15	1.5	200	10	0.4	0.291	0.3772
27	−1	0	0	1	0	5	1.5	200	30	0.4	0.172	0.2712
28	1	0	0	1	0	15	1.5	200	30	0.4	0.755	0.3905
29	0	0	−1	0	−1	10	1.5	100	20	0.2	0.476	0.3136
30	0	0	1	0	−1	10	1.5	300	20	0.2	0.39	0.3561
31	0	0	−1	0	1	10	1.5	100	20	0.6	0.429	0.2565
32	0	0	1	0	1	10	1.5	300	20	0.6	0.751	0.3428
33	−1	0	0	0	−1	5	1.5	200	20	0.2	0.39	0.3116
34	1	0	0	0	−1	15	1.5	200	20	0.2	0.432	0.3847
35	−1	0	0	0	1	5	1.5	200	20	0.6	0.214	0.3033
36	1	0	0	0	1	15	1.5	200	20	0.6	0.781	0.4267
37	0	−1	0	−1	0	10	1.0	200	10	0.4	0.451	0.361
38	0	1	0	−1	0	10	2.0	200	10	0.4	0.36	0.3205
39	0	−1	0	1	0	10	1.0	200	30	0.4	0.417	0.3303
40	0	1	0	1	0	10	2.0	200	30	0.4	0.412	0.3293
41	0	0	0	0	0	10	1.5	200	20	0.4	0.453	0.3315
42	0	0	0	0	0	10	1.5	200	20	0.4	0.523	0.3338
43	0	0	0	0	0	10	1.5	200	20	0.4	0.439	0.3271
44	0	0	0	0	0	10	1.5	200	20	0.4	0.396	0.3309
45	0	0	0	0	0	10	1.5	200	20	0.4	0.383	0.3183
46	0	0	0	0	0	10	1.5	200	20	0.4	0.371	0.3585

Table 4. ANOVA results for predictive models.

Source	DoF	SS	Contr., %	Adj. MS	*F*-value	*P*-value
(a) Surface roughness (Ra) model						
Model	20	0.979426	88.92%	0.048971	10.03	<0.00001
Linear	5	0.576319	52.32%	0.115264	23.60	<0.00001
DC	1	0.420293	38.16%	0.420293	86.06	<0.00001
GV	1	0.023639	2.15%	0.023639	4.84	0.037
T_{ON}	1	0.01409	1.28%	0.014090	2.88	0.102
T_{OFF}	1	0.05611	5.09%	0.056110	11.49	0.002
FP	1	0.062188	5.65%	0.062188	12.73	0.001
Square	5	0.139988	12.71%	0.027998	5.73	0.001
DC*DC	1	0.032140	4.79%	0.032140	6.58	0.017
GV*GV	1	0.014340	3.33%	0.014340	2.94	0.099
TON*TON	1	0.000899	0.11%	0.000899	0.18	0.672
TOFF*TOFF	1	0.005421	0.02%	0.005421	1.11	0.302
FP*FP	1	0.049099	4.46%	0.049099	10.05	0.004
2-Way Interaction	10	0.263119	23.89%	0.026312	5.39	<0.00001
DC*GV	1	0.034969	3.17%	0.034969	7.16	0.013
DC*TON	1	0.011578	1.05%	0.011578	2.37	0.136
DC*TOFF	1	0.065792	5.97%	0.065792	13.47	0.001
DC*FP	1	0.068906	6.26%	0.068906	14.11	0.001
GV*TON	1	0.000324	0.03%	0.000324	0.07	0.799
GV*TOFF	1	0.001849	0.17%	0.001849	0.38	0.544
GV*FP	1	0.000020	0.00%	0.000020	0.00	0.949
TON*TOFF	1	0.030276	2.75%	0.030276	6.20	0.020
LR-TON*FP	1	0.041616	3.78%	0.041616	8.52	0.007
TOFF*FP	1	0.007788	0.71%	0.007788	1.59	0.218
Error	25	0.122096	11.08%	0.004884		
Lack-of-Fit	20	0.106029	9.63%	0.005301	1.65	0.304
Pure Error	5	0.016067	1.46%	0.003213		
Total	45		100.00%			
Source	DoF	Adj. SS	Contr., %	Adj. MS	*F*-value	*P*-value
(b) Overcut (OC) model						
Model	20	0.090892	93.69%	0.004545	18.55	<0.00001
Linear	5	0.058467	60.26%	0.011693	47.73	<0.00001
DC	1	0.036015	37.12%	0.036015	147.02	<0.00001
GV	1	0.004855	5.00%	0.004855	19.82	<0.00001
T_{ON}	1	0.016796	17.31%	0.016796	68.57	<0.00001
T_{OFF}	1	0.000486	0.50%	0.000486	1.98	0.171
FP	1	0.000315	0.32%	0.000315	1.29	0.268
Square	5	0.014488	14.93%	0.002898	11.83	<0.00001
DC*DC	1	0.006074	9.63%	0.006074	24.80	<0.00001
GV*GV	1	0.000844	2.60%	0.000844	3.44	0.075
TON*TON	1	0.000395	0.01%	0.000395	1.61	0.216
TOFF*TOFF	1	0.002200	1.62%	0.002200	8.98	0.006
FP*FP	1	0.001033	1.06%	0.001033	4.22	0.051
2-Way Interaction	10	0.017938	18.49%	0.001794	7.32	<0.00001
DC*GV	1	0.004949	5.10%	0.004949	20.20	<0.00001
DC*TON	1	0.004775	4.92%	0.004775	19.49	<0.00001
DC*TOFF	1	0.000821	0.85%	0.000821	3.35	0.079

Table 4. (continued).

Source	DoF	SS	Contr., %	Adj. MS	*F*-value	*P*-value
DC*FP	1	0.000633	0.65%	0.000633	2.58	0.121
GV*TON	1	0.000001	0.00%	0.000001	0.00	0.947
GV*TOFF	1	0.000390	0.40%	0.000390	1.59	0.219
GV*FP	1	0.000289	0.30%	0.000289	1.18	0.288
TON*TOFF	1	0.004469	4.61%	0.004469	18.24	0.000
TON*FP	1	0.000480	0.49%	0.000480	1.96	0.174
TOFF*FP	1	0.001132	1.17%	0.001132	4.62	0.041
Error	25	0.006124	6.31%	0.000245		
Lack-of-Fit	20	0.005216	5.38%	0.000261	1.44	0.367
Pure Error	5	0.000908	0.94%	0.000182		
Total	45		100.00%			

surface roughness of machined component, as supported and justified by F-statistics (86.06) and *P*-value (<0.00001). The factors such as, pulse-on-time and interactions (DC*TON, GV*TON, GV*TOFF, GV*FP, TOFF*FP) reflect insignificant impact on Ra, as their contributions are very inconsiderable. In the same context, the ANOVA result of overcut (OC) model is presented in Table 4b, which shows the *P*-value is desirable (i.e., under 0.05), thereby resulting in excellent significance of regression model. It was observed that (see Tab. 4b) among the several process parameters that have been considered during machining of aluminum-silicon carbide metal matrix composite, the terms DC, GV, TON, DC*DC, TOFF*TOFF, DC*GV, DC*TON, TON*TOFF and TOFF*FP are found to be significant at 95% confidence level as well as are the influencing parameters of OC. The other parameters don't present statistical significance as well as an important role on OC because of their larger *P*-value, and the calculated *F*-value is not more than *F*-value. Considering the criterion of significant level to 0.05 and the insight of the *F*-value reveals that the individual effect of discharge current (DC) has the dominant contributor on overcut of machined hole, which explains the larger calculated *F*-values than standardized F-distribution value.

To avoid the misleading conclusion, different diagnostic tests such as adequacy, effectiveness and goodness-of-fit were carried out for developed regression models (Ra and OC). When the regression coefficient (R^2-value) approaches to one, the predicted model effectively fits with the actual data. For surface roughness and overcut models, the calculated R^2-values (0.889 and 0.936, respectively) are very close to unity, which depicts statistical significance as well as goodness-of fit for the proposed model. Moreover, there is a very good degree of resemblance between the experimental and predicted value, as shown in Figure 3. Thus, it is concluded that the proposed model has high effectiveness with good predictability. From the normal probability plot (see Fig. 4), it is noticed that all the terms related with the regression model of Ra and OC are statistically significant as the residuals are approaching to a straight line, which concluded that associated errors were normally distributed. With lower AD-statistic (0.725 for Ra, and 0.435 in case of OC) as well as larger *P*-value (0.055 for Ra, and 0.288 in case of OC) received from Anderson-Darling test, confirmed that null-hypothesis can't be rejected. Finally, it is concluded that, the proposed predictive models for surface roughness and overcut using RSM is efficient, statistically significant, adequate and also probabilistically validate as it has low probability value (less than 0.05), higher R^2-value and larger AD-test *P*-value.

3.2 Parametric influence on technological responses

The effect of process parameters (discharge current, gap voltage, pulse-off-time, pulse-on-time, and flushing pressure) on two major technological responses (Ra, OC) of machined part quality are graphically analyzed by three-dimensional (3D) surface plot. Figure 5a illustrates the combined effect of increasing discharge current and gap voltage on surface roughness, Ra. Higher discharge current gives rise to higher discharge spark energy as well as current density. Consequently, increasing MRR results in bigger-deeper carter marks on the machined surface and hence, poor surface finish. Almost the same effect is also observed when spark voltage is raised. Figure 6 shows the SEM micrograph of machined component having poor surface quality that explains the topographical status in terms of crater (due to the existence of different kinds of interaction among the dielectric circulations, debris, and continuous electrical discharge spark), globular modules of debris (attributed to cohesion effect in the machined surface caused by molten material, cold welding effects, and insufficient flushing of dielectric fluid in the gap), micro-voids (due to the gas produced in the discharge process), micro-crack (attributed to the overreach of induced stress over the tensile strength of the workpiece material caused by rapid heating and cooling effect), and micro-pores (due to low fracture toughness and thermal shock resistance of Al-SiC MMC). Moreover, it is observed that, with increased discharge current under machining condition (GV = 2 V; TON = 200 µs; TOFF = 20 µs; FP = 0.2 kgf/cm^2) transferring more thermal energy that

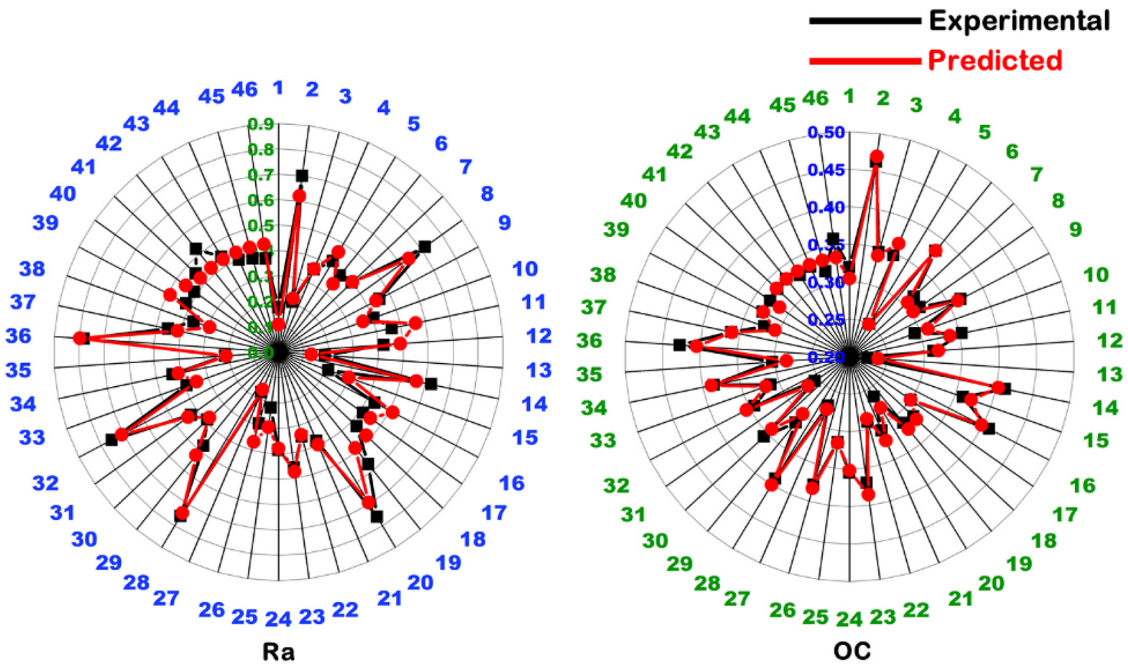

Fig. 3. Comparison between experimental and predicted values of technological parameters: (a) surface roughness, and (b) overcut.

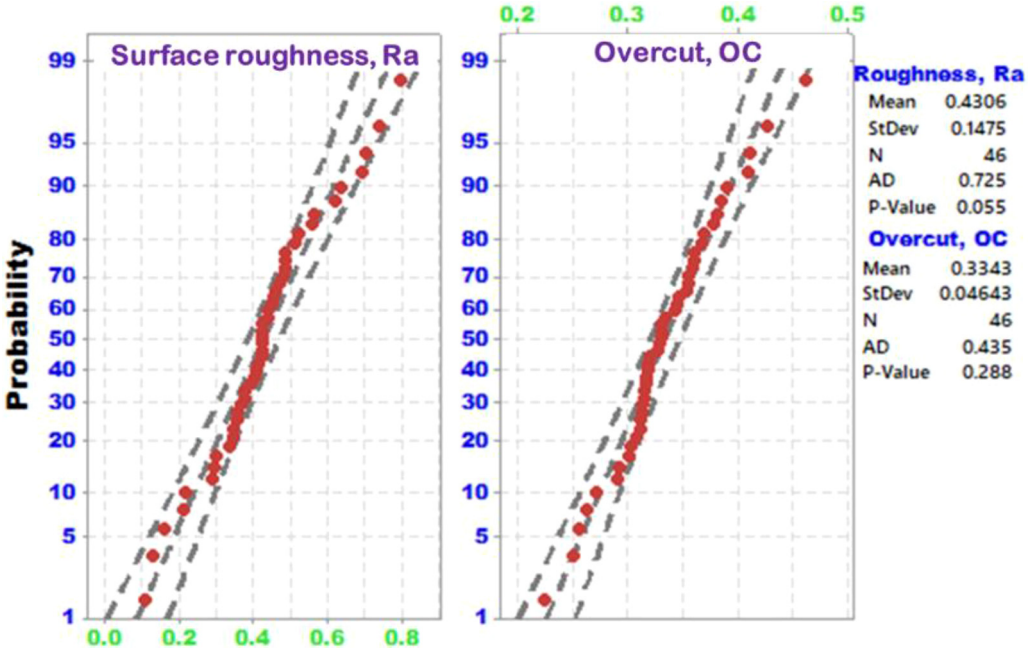

Fig. 4. Normal probability plot for responses (Ra, OC).

develops extremely high temperature at the target surface where the spark strikes cause melting followed by vaporization of MMC material and induces undesirable deep-irregular on workpiece surface, thereby resulting poor surface finish. Figure 7 shows the SEM microphotograph of machined surface under the influence of different discharge currents. It is obvious form these images that, increase of discharge energy aids in the enlarging and deepening of the crater size, which comes with other surface defects such as micro cracks. Therefore, larger discharge energy hinders the surface integrity and to some extent compromises its application capability. Increasing pulse-on-time, at higher pulse-off-time, as shown in Figure 5b, results in increase in surface roughness. This is because the energy available for material removal during a given period is shared less by a large number of sparks; hence the corresponding crater size is increased. Moreover, shorter the pulse-on-time removes very little metal, closer to the accuracy with less thermal damage to the workpiece produces better surface finish, Ra. Apart effect of flushing pressure seems to be insignificant

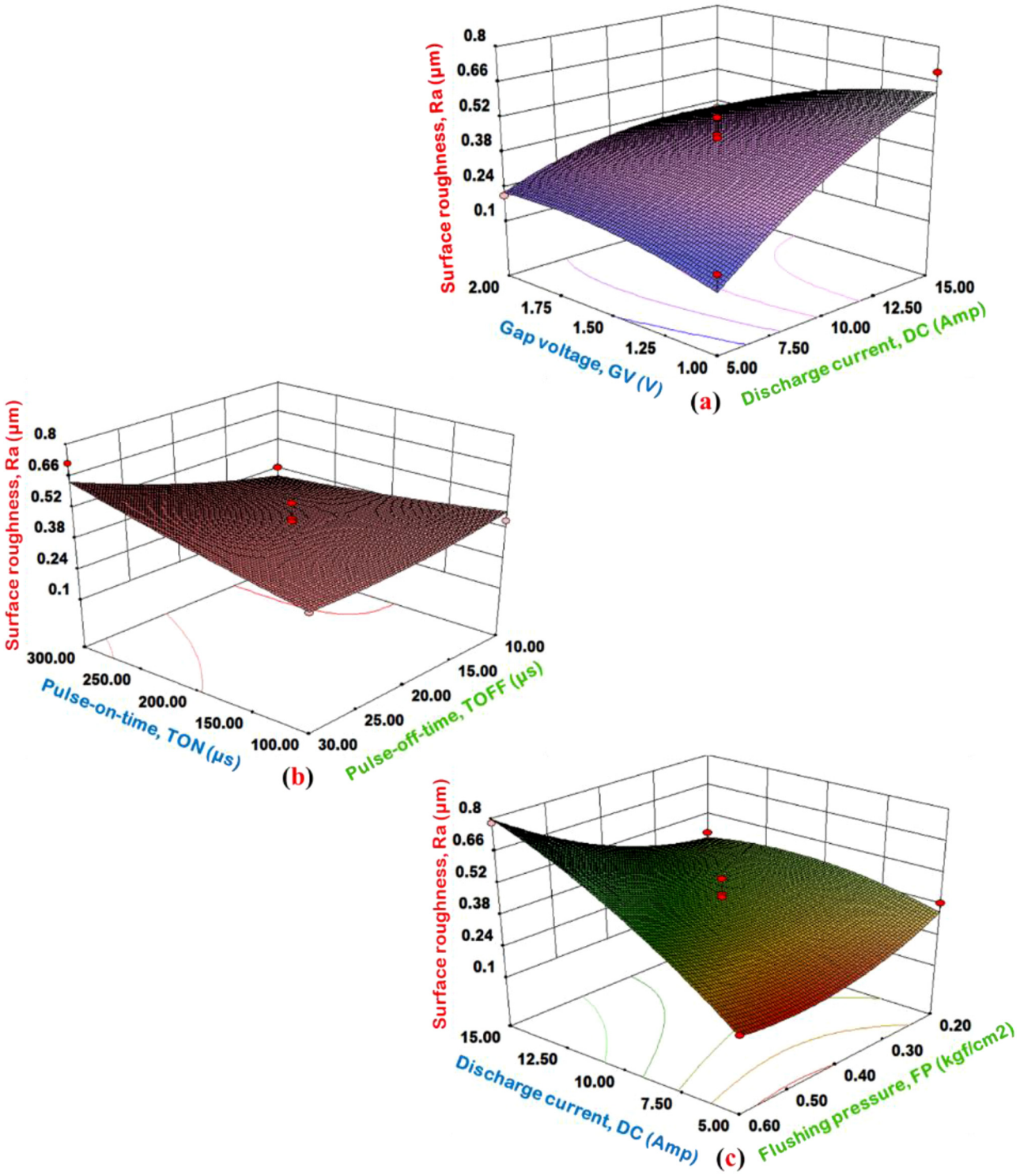

Fig. 5. Surface plots for illustration of machining parameters effect on surface roughness.

on surface finish of the machined part, as shown in Figure 5c. However, it is advisable to keep suitable flushing pressure during electrical discharge machining to prevent stagnation of dielectric fluid and short circuit.

During EDM, the role of dielectric fluid is to flush out the molten material away from the work surface, which is under melting (or partial melting) condition. While flushing, molten material is transformed into tiny particles (droplets), which are expected to be carried away; thereby, exposing a new layer. But all the particles are not flushed out, and they adhere to the top surface of the machined workpiece due to evaporation of the dielectric fluid. That part of the molten material appearing on the topmost layer is known as re-solidified layer; also called as recast layer

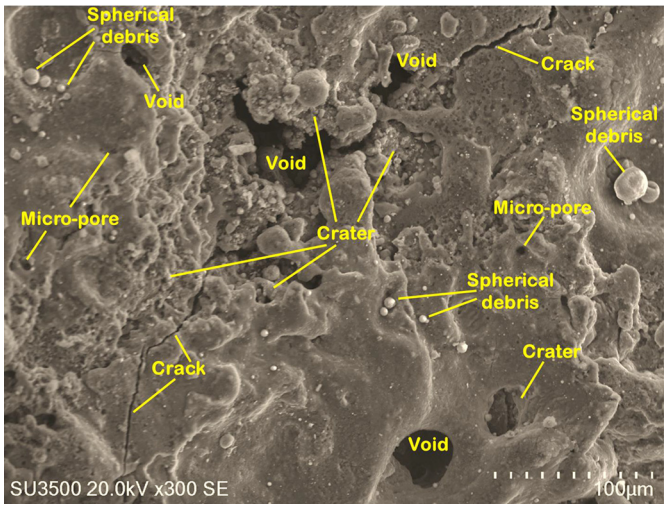

Fig. 6. SEM images of poor surface quality of machined component at DC = 15 amp, GV = 1.5 V, TON = 200 μs, TOFF = 20 μs, and FP = 0.6 kgf/cm^2.

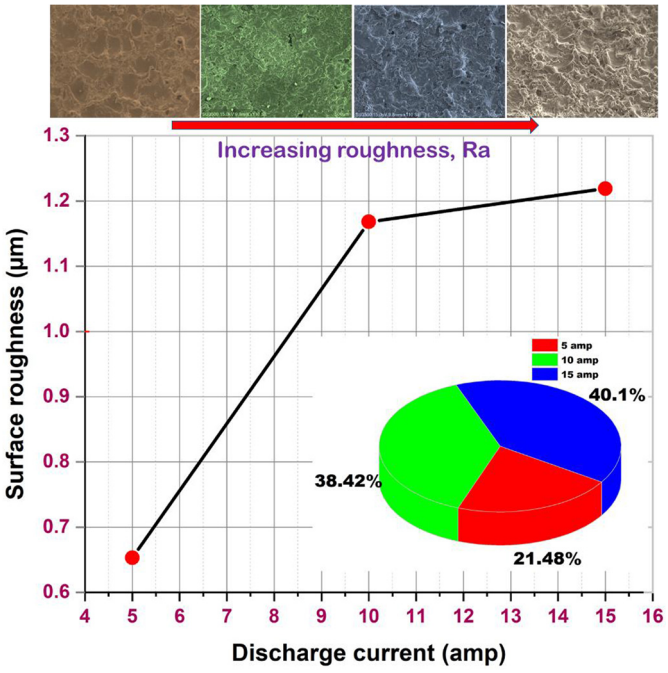

Fig. 7. Influence of discharge current on radial overcut of machined hole at GV = 2 V; TON = 200 μs; TOFF = 20 μs; FP = 0.2 kgf/cm^2.

[48]. This layer exhibits brittleness to a large extent. Figure 8 depicted the existence of recast layer as noticed from SEM micrographs of machined Al-SiC MMC at parameters setting: GV = 2 V; TON = 200 μs; TOFF = 20 μs; FP = 0.2 kgf/cm^2. It is also observed that the thickness of recast layer had an increasing trend with an increase in the discharge current.

Figures 9a and 9b illustrate the influence of discharge current and pulse-on-time on overcut (OC). The effect of above-mentioned two parameters leads to the increase in discharge energy per every individual spark, as well as cutting time along with cutting velocity, and consequently transfers more thermal energy on workpiece surface that results in more evaporation of material in comparison to sub-surface and in turn it affects increase in dimensional deviation of hole, especially radial overcut caused by side spark erosion [49]. Moreover, it is observed that, with increased discharge current under cutting condition (GV = 1 V; TON = 200 μs; TOFF = 20 μs; FP = 0.4 kgf/cm^2) results in increased overcut, presented in Figure 10. In fact, overcut increases with an increase in flushing pressure upto certain point then decrease, as shown in Figure 9c. Similar observation has been reported on overcut in electrical discharge machining of SS316 [50]. The overcut reduces with increase in pressure upto 0.4 kgf/cm^2 can simply be illustrated as a consequence of less deposition of debris elements in the machining zone, which develops uniformity of sparking at the periphery of machined surface (i.e. wall-edge at the entrance of machined hole). Nevertheless, more increase in flushing pressure promotes increase in OC which can be explained due to a reduction in flushing effectiveness as the density of the debris particles are too high at certain points within the gap. Figure 11a shows the SEM images of cross-section view for the side wall of machined hole formed by EDM with various discharge current. It is noticed that at lower value of DC, the side wall of machined hole generated on Al-SiC MMC is recommended than that one achieved by machining with a higher discharge current. The reason is that at lower value of DC, the current density is not so much during pulse-on-time, that resulting in less electrode (tool) wear and hence, the improved hole quality. Moreover, it is evidenced that hole taper gradually increases with the rise in discharge current from 5 to 15 amp may be attributed to the fact that thermal energy per unit area is more which might have resulted in high tool wear causing deterioration of tool-tip geometry and thus, resulting geometrical deviation of hole in the form of increased hole taper. Optical micrographs (see Fig. 11b) exhibiting the size of craters formed at various discharge current is evaluated quantitively using a circle to surround the crater marks. It is observed that while executing EDM of Al-SiC MMC, increase in peak discharge current, the crater size increased and resulting in the reduced hole quality in the form of poor surface finish of the hole side wall. Thereby resulting geometric shape deformation of hole as increased overcut.

During electrical discharge machining, intense heat is produced on the workpiece surface because of the spark discharge for which material removal is caused in views of melting followed by evaporation. However, the spark not only melts the workpiece but also melts the tool electrode too. The melting of the tool is called electrode wear. Tool wear rate is considerably affected by specific heat capacity, melting point and thermal conductivity of the electrode material. In addition, dielectric medium circulation flow rate and tool geometry also partly responsible for tool wear. The microscopic view of the bottom surface as well as edge of tool electrode after EDM operation on Al-SiC MMC are presented in Figure 12. Carbon deposition is noticed both at the bottom surface and around the edge of the tool electrode. It is also observed from the optical images that,

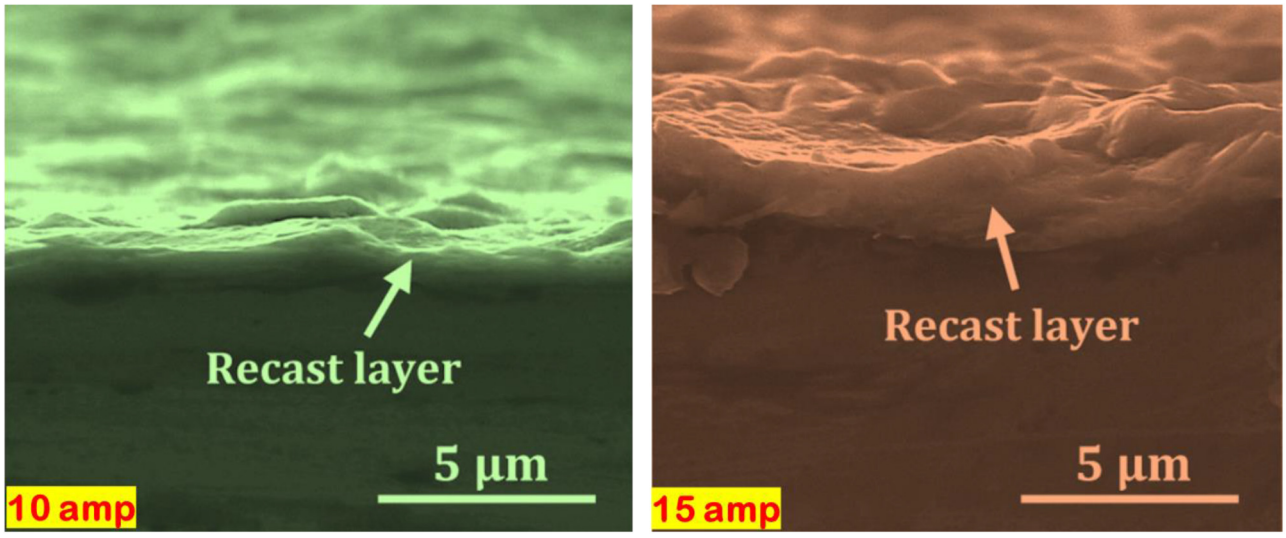

Fig. 8. Cross-sectional SEM images of machined surfaces showing an increase in recast layer thickness with discharge current.

increase in discharge current results in increased tool wear (obtained at parameters setting: GV = 1 V; TON = 200 μs; TOFF = 20 μs; FP = 0.4 kgf/cm^2). This is so because, during electrical discharge machining, heat is mostly transferred to both the tool electrode and work surfaces. Pyrolysis of the dielectric liquid medium produces pyrolytic carbon atoms, which gets deposit on bottom as well as edge of the tool (and at the machined surface as well), developing a blackish layer of carbides. Deposition of hard and low-conductive carbide layer lowers the thermal conductivity of tool electrode as a whole. These issues promote the electrode wear. Particularly, such carbides accumulated at the tool surface serve as a heat conductive barrier. Thus, heat can only be transferred through bulk of the electrode material after this barrier is overcome. This illustrates the mechanism of tool wear, and leads to poor electrode shape retention capability.

3.3 Optimization using response surface methodology

The present study includes multiple-response optimization based on the desirability function approach of RSM, to keep the surface roughness as well as overcut of machined hole to the minimum. Parameter design is an effective way to improve product quality as well as the process efficiency. Desirability function approach is a statistical based multiple response robust parameter design methodology, employed for solving the multi-objective optimization problems. The approach looks for correct combination of parameter levels that simultaneously takes the responsibility to fulfill the requirements placed on each response. The criterion for achievement of optimization result is evaluated based on overall desirability, which is a weighted geometric mean of respective desirability for the different performance characteristics, which are expressed within the range of 0–1. The response will be completely unaccepted or undesirable if the desirability value approaches to 0. Response will be most desirable or accepted only if the ideal desirability value is near or equal to 1.

For solving the parameter design problems by desirability function approach, the objective function, F(x) is specified as [51];

$$F(x) = -\mathrm{DF}$$

Overall (i.e. composite) desirability function can be stated as;

$$\mathrm{DF} = \left(\prod_{i=1}^{n} d_i^{w_i}\right)^{\frac{1}{\sum_{j-1}^{n} w_i}} \tag{3}$$

Here, DF is the composite desirability function which finds the optimal setting by minimizing the $F(x)$ (i.e. maximizes DF as it is highly desirable for optimization), d_i is the desirability designated for the i^{th} targeted output, and w_i is the weighting of d_i (considered equally important) in this study.

For a goal to minimization of output, individual desirability can be defined as;

$$\begin{aligned} d_i &= 1 \text{ if } Y_i \leq L_{i.} \\ d_i &= \left[\frac{H_i - Y_i}{H_i - L_i}\right] \text{ if } L_i \leq Y_i \leq H_i \\ d_i &= 0 \text{ if } Y_i \geq H_i \end{aligned} \tag{4}$$

where L_i and the H_i are the lowest and largest acceptable value of Y for the i^{th} output response respectively.

The optimal solution was obtained using Design Expert 11 software. A set of thirty-six solutions were obtained, and the solution with the highest desirability (close to 1) was selected, as shown in the ramp function graph in Figure 13a. Once the optimal level of process parameters is selected, the final step to predict and verify the improvement of the performance characteristics using the optimal level of the machining parameters. The point on the graph shows the optimal values for the responses and the height obtained for each point in the graph discloses

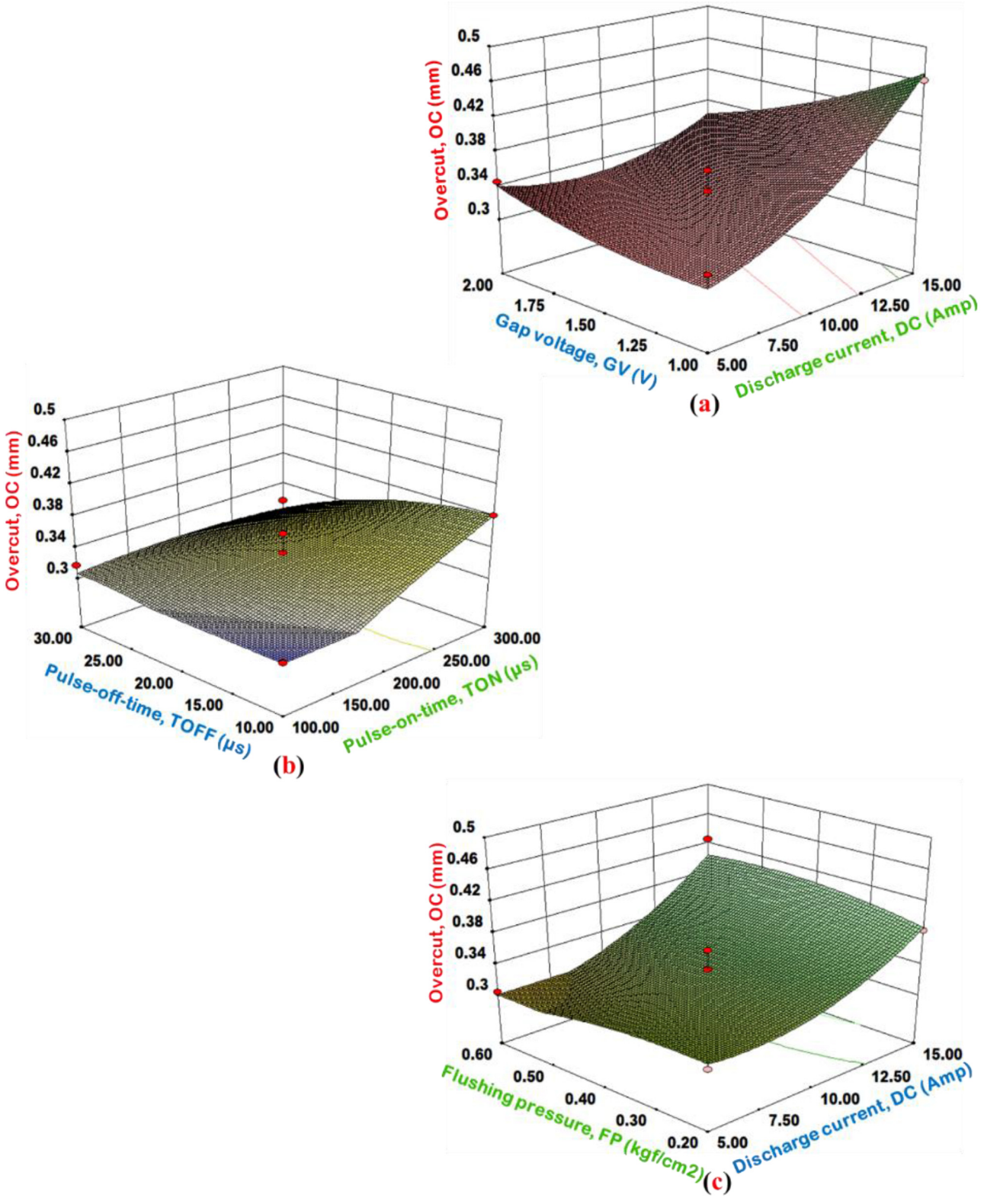

Fig. 9. Surface plots for illustration of machining parameters effect on overcut.

how much enviable are the optimal values obtained. These values were validated by conducting confirmation experiments. The values for the optimal parameters are derived from the points on the ramp graphs. Figure 13b shows optimization plot based on desirability function approach for technological responses, showing the optimal manufacturing conditions for electrical discharge machining of Al-SiC MMC with discharge current (DC) of

5.12 amp, gap voltage (GV) of 1.95 V, pulse-on-time (TON) of 100.02 µs, pulse-off-time (TOFF) of 12.45 µs, and flushing pressure (FP) of 0.55 kgf/cm^2. Finally, the estimated optimal values of pre-cited two technological responses are 0.17032 µm for Ra, and 0.22412 mm in case of OC.

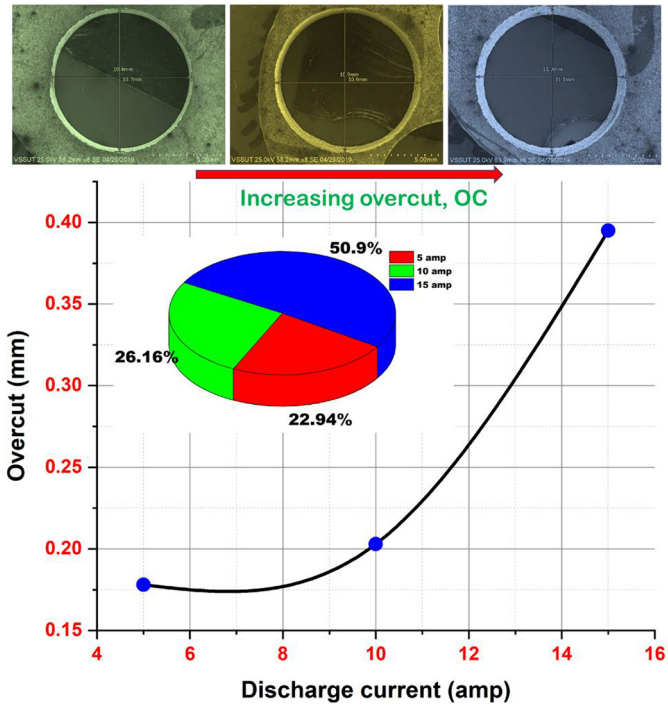

Fig. 10. Influence of discharge current on radial overcut of machined hole at GV = 1 V; TON = 200 µs; TOFF = 20 µs; FP = 0.4 kgf/cm^2.

3.4 Confirmation test

With a view to avoid the misleading conclusion, the optimum machining conditions suggested by desirability function analysis of RSM technique are validated with the results of confirmation test, which could be possible by conducting one additional experiment using the same experimental setup. A comparison between the optimal and experimental values of responses (Ra, OC) under the cutting conditions proposed by RSM is presented in Table 5. The results of RSM approach presents the suitable combination of machining parameters for optimization of surface roughness and overcut because the error percentage is lower (5.8%). Hence, the optimization results obtained by RSM approach is considered for cost analysis.

3.5 Cost analysis

Cost consciousness with respect to machining process is a fundamental venture in efficient manufacturing system. In order to determine the manufacturing cost for a machining operation, important criteria are selected based on convolution of shape, product accuracy and tooling process. Nowadays, with increased pressure on profitability and cost management, manufacturers decided to standardized the total cost in machining operation to ensure consistency and set cost benchmarks for future reference. Because of the large expenditures involved, it is a prime importance to analyze machining operations in order to operate with optimum economic conditions. For components produced by machining, cost estimation is kept minimum by considering the optimum cutting condition and total machining cost per part. This means appropriate selection of machining parameters will definitely affect the

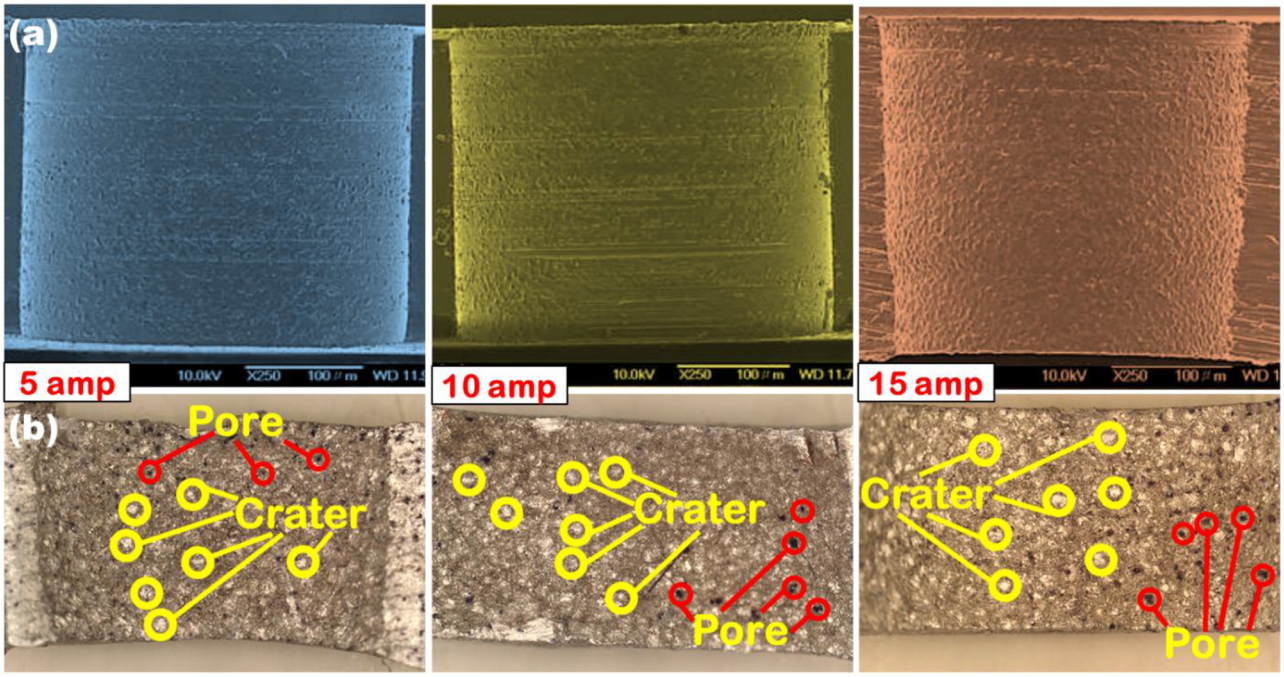

Fig. 11. Influence of peak discharge current on hole quality formed by EDM at GV = 1V; TON = 200 µs; TOFF = 20 µs; FP = 0.4 kgf/cm^2.

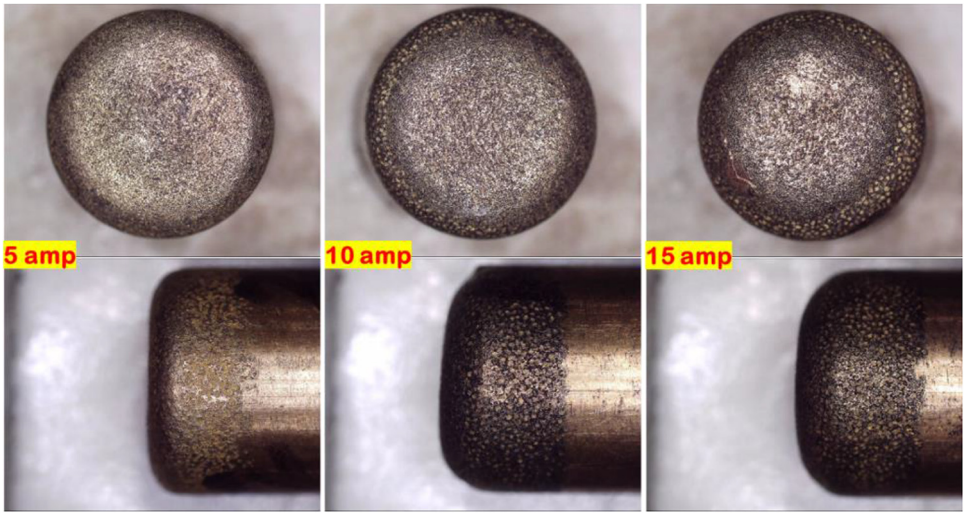

Fig. 12. Deposition of carbon layer at the bottom and edge of the tool electrode after EDM on Al-SiC MMC workpiece at GV = 1 V; TON = 200 µs; TOFF = 20 µs; FP = 0.4 kgf/cm^2.

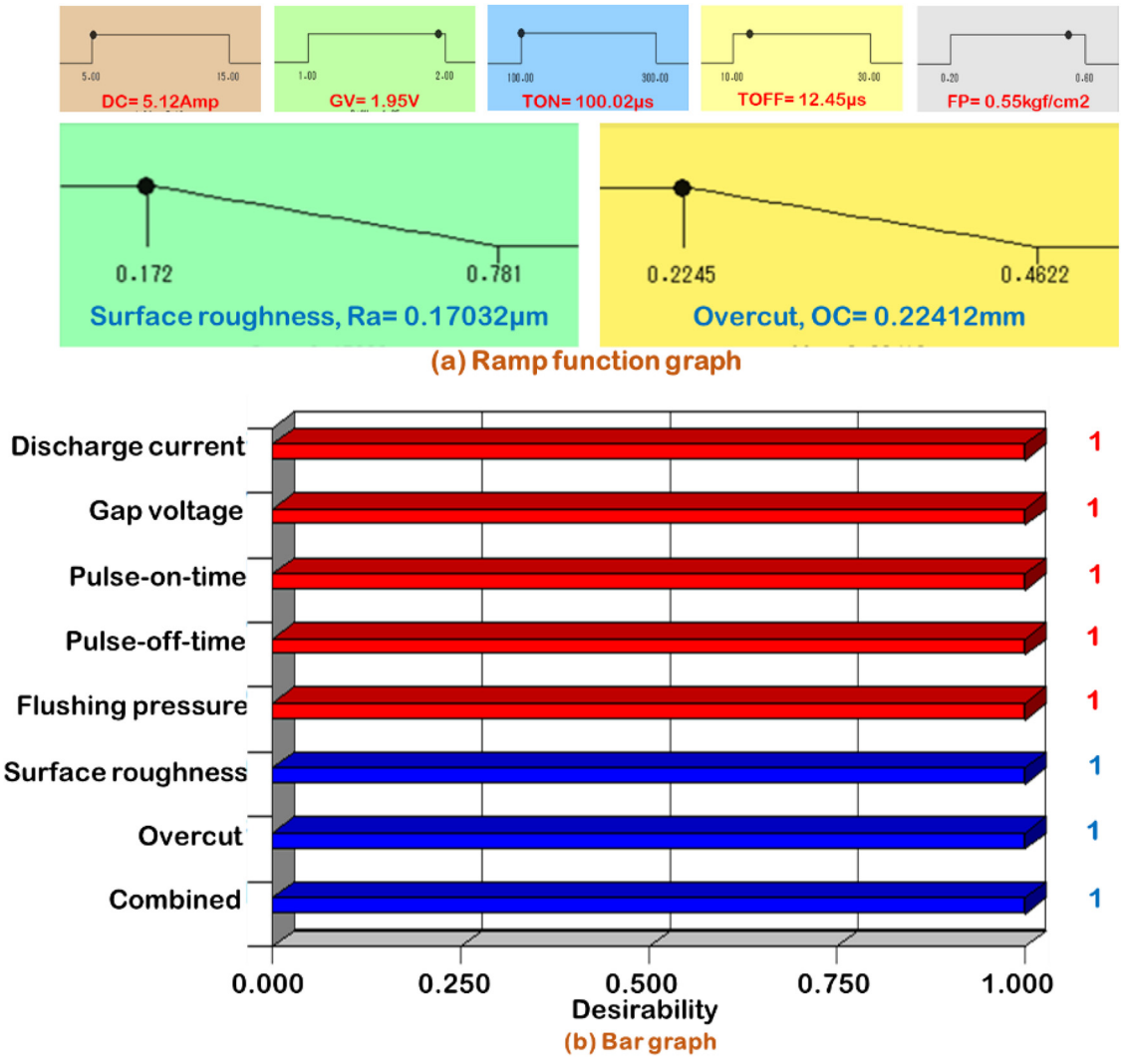

Fig. 13. Optimization plot for surface roughness and overcut using desirability function approach.

Table 5. Overview of confirmatory test results.

Optimum machining parameters					Surface roughness, Ra (μm)		Overcut, OC (mm)		Average error (%)
DC	GV	TON	TOFF	FP	Predicted	Experimental	Predicted	Experimental	
5	2	100	12.5	0.55	0.17032	0.182	0.2241	0.2374	5.8%

Table 6. Cost estimation in electrical discharge machining of Al-SiC MMC.

Specific basic variables	In minutes	Costs	In Indian rupees
Workpiece clamping and positioning time, T_{clamp}	5	Cost of each electrode, C_{elcd}	Rs.15
Electrode positioning and zeroing time, T_p	1	Cost of machine working per minute, $C_{\text{mach/min}}$	Rs.8.33
Electrode drawing out time, T_{edr}	1	Cost of machine operator per minute, $C_{\text{op/min}}$	Rs.5.83
Single hole drilling time at optimum machining conditions, T_d	11.5	Total machining cost per component, C_{tot} $\{(C_{\text{elcd}}) + (T_{\text{tot}}{}^{*}C_{\text{mach/min}}) + [(T_{\text{clamp}} + T_{\text{edr}})^{*}1.2^{*}C_{\text{op/min}}]\}$	Rs. 211.08
Total machining time per component, T_{tot} $(T_{\text{clamp}} + T_p + T_{\text{edr}} + T_d)$	18.5		

production rate as well as manufacturing cost. Considering the optimal cutting conditions suggested by RSM technique, cost analysis is used to perform detailed direct and indirect cost estimation in terms of total machining cost per part in electrical discharge machining process [52], as shown in Table 6. It is noticed that the total machining cost per part in electrical discharge machining is considerably lower around Rs.211.08 at optimum condition. It is interesting to note that the cost estimation of operational activities in EDM process ensures a dramatic gain in productivity and efficiency in finish machining. The cheapest solution to the total machining cost per part, longer tool life with minimized downtime calculations is obtained using brass as electrode material that justifies an economic solution to machining of Al-SiC MMC.

4 Conclusions

In the present experimental investigation, predictive modelling and multi-response optimization of EDM process is done for Al-SiC MMC with brass electrode by the combined approach of Box Behnken design (BBD) – analysis of variance (ANOVA), response surface methodology (RSM) and desirability function analysis (DFA) to analyze the surface roughness and overcut. Also, an economic analysis is performed to estimate the total machining cost per component during EDM of Al-SiC MMC. The following conclusions are obtained.

- The contribution of discharge current is found to be the most responsible factor for the degradation of surface quality as well as finish, and achieved the roughness (R_a) in the range of 0.172–0.781μm.
- ANOVA analysis followed by the 3D surface effect plot illustrated that, the discharge current followed by pulse-on-time are the influential parameters to control the dimensional deviation of hole diameter, i.e. overcut (OC) produced by electrical discharge machining.
- Result showed that discharge current has the significant contribution (38.16% for Ra, 37.12% in case of OC) in degradation of surface finish as well as dimensional deviation of hole diameter, especially overcut.
- Topological as well as morphological status of the machined Al-SiC MMC surface is observed indeed disappointing due to the presence of crater marks, uneven fusion structure, globules of debris, voids and surface microcracks. Recast layer is found at the top of the machined surface. However, intensity of surface irregularities, thickness of recast layer are observed increasing with increase in discharge current.
- Dielectric cracking also results in deposition of hard carbide layer at the bottom of the tool electrode. Formation of such carbide layer is detrimental since it promotes rapid tool wear hence adversely affecting tool shape retention capability as well as corner size machining accuracy.
- The predictive models for various technological parameters developed by RSM technique are found to be adequate, statistically significant and probabilistically valid because their higher R^2-value (0.889 and 0.936, respectively for Ra and OC), model probability P-value under 0.05 and larger AD-test P-value (0.055 and 0.288, respectively for Ra and OC).
- The application of RSM's desirability function analysis for multi-response optimization presented the optimal manufacturing conditions for electrical discharge machining of Al-SiC MMC at discharge current (DC) of 5.12 amp, gap voltage (GV) of 1.95V, pulse-on-time (TON) of 100 μs, pulse-off-time (TOFF) of 12.45 μs, and flushing pressure (FP) of 0.55 kgf/cm^2. The estimated optimum value of technological responses is 0.17032μm for Ra, and 0.22412mm in case of OC.

– At optimal conditions (suggested by RSM technique), the estimated total machining cost per component of only Rs.211.08 in Indian rupees, ensures benefit from economical point of view because of reduced machining time and machine downtime.
– The proposed multiple techniques demonstrate an effective approach towards improvement in EDM process and it can be implemented in real-time process monitoring, predictive model control and optimization during machining of different workpiece materials as well as in other machining processes via. advances in computer technology.

In terms of future work, this study can be extended to analyze the influence of tool material as well as the type of dielectric fluids to improve the surface quality and reduced overcut. Further investigations can be carried out to assess the effects of EDM process parameters on tool wear rate (TWR) and material removal rate (MRR).

Nomenclature

ϕ	Diameter in mm
R_a	Arithmetic average surface roughness in μm
R^2	Coefficient of determination
T_{clamp}	Workpiece clamping and positioning time in minute
Tp	Electrode positioning and zeroing time in minute
T_{edr}	Electrode drawing out time in minute
T_d	Single hole drilling time at optimum machining conditions in minute
T_{tot}	Total machining time per component in minute
C_{elcd}	Cost of each electrode in rupees
$C_{\text{mach/min}}$	Cost of machine working per minute in rupees
$C_{\text{op/min}}$	Cost of machine operator per minute in rupees
C_{tot}	Total machining cost per component in rupees
EDM	Electrical discharge machining
Al-SiC	Aluminium-silicon carbide
MMC	Metal matrix composite
DC	Discharge current in ampere
GV	Gap voltage in volt.
T_{ON}	Pulse-on-time in μs
T_{OFF}	Pulse-off-time in μs
FP	Flushing pressure in kgf/cm^2
OC	Overcut in mm
BBD	Box-Behnken design
RSM	Response surface methodology
ANN	Artificial neural network
GA	Genetic algorithm
GRA	Grey relational analysis
ANOVA	Analysis of variance
SS	Sum of squares
MS	Mean of squares
SEM	Scanning electron microscope
PSO	Particle swarm optimization

References

1. B. Mohan, A. Rajadurai, K.G. Satyanarayana, Electric discharge machining of Al-SiC metal matrix composites using rotary tube electrode, J. Mater. Process. Technol. **153–154** (2004) 978–985
2. D. Kanagarajan, R. Karthikeyan, K. Palanikumar, P. Sivaraj, Influence of process parameters on electric discharge machining of WC/30%Co composites, Proc. Inst. Mech. Eng. B **222** (2008) 807–815
3. V. Gohil, Y.M. Puri, Statistical analysis of material removal rate and surface roughness in electrical discharge turning of titanium alloy (Ti-6Al-4V), Proc. Inst. Mech. Eng. B **232** (2016) 1603–1614
4. O. Belgassim, A. Abusaada, Investigation of the influence of EDM parameters on the overcut for AISI D3 tool steel, Proc. Inst. Mech. Eng. B **226** (2011) 365–370
5. C.P.M. Mohanty, P.S. Satpathy, S. Mahapatra, M.R. Singh, Optimization of cryo-treated EDM variables using TOPSIS-based TLBO algorithm, Sādhanā **43** (2018) 51
6. C.P.S. Mohanty, S. Mahapatra, M.R. Singh, An intelligent approach to optimize the EDM process parameters using utility concept and QPSO algorithm, Eng. Sci. Technol. **20** (2017) 552–562
7. S.H. Lee, X.P. Li, Study of the effect of machining parameters on the machining characteristics in electrical discharge machining of tungsten carbide, Journal of Materials Processing Technology **115** (2001) 344–358
8. M. Bhaumik, K. Maity, Effect of different tool materials during EDM performance of titanium grade 6 alloy, Eng. Sci. Technol. **21** (2018) 507–516
9. D. Rahul, K. Mishra, S. Datta, M. Masanta, Effects of tool electrode on EDM performance of Ti-6Al-4V, Silicon **10** (2018) 2263–2277
10. M.H. Raza, A. Wasim, M.A. Ali, S. Hussain, M. Jahanzaib, Investigating the effects of different electrodes on Al6061-SiC-7.5 wt% during electric discharge machining, Int. J. Adv. Manufactur. Technol. **99** (2018) 3017–3034
11. S. Kumari, S. Datta, M. Masanta, G. Nandi, P.K. Pal, Electro-discharge machining of Inconel 825 super alloy: effects of tool material and dielectric flushing, Silicon **10** (2018) 2079–2099
12. M.B.A. Ndaliman, A. Khan, M.Y. Ali, Influence of dielectric fluids on surface properties of electrical discharge machined titanium alloy, Proc. Inst. Mech. Eng. **227** (2013) 1310–1316
13. Y. Zhang, Y. Liu, Y. Shen, R. Ji, Z. Li, C. Zheng, Investigation on the influence of the dielectrics on the material removal characteristics of EDM, J. Mater. Process. Technol. **214** (2014) 1052–1061
14. P. Sadagopan, B. Mouliprasanth, Investigation on the influence of different types of dielectrics in electrical discharge machining, Int. J. Adv. Manufactur. Technol. **92** (2017) 277–291
15. C. Li, X. Xu, Y. Li, H. Tong, S. Ding, Q. Kong, L. Zhao, J. Ding, Effects of dielectric fluids on surface integrity for the recast layer in high speed EDM drilling of nickel alloy, J. Alloys Compd. **783** (2019) 95–102
16. K.-T. Chiang, F.-P. Chang, D.-C. Tsai, Modeling and analysis of the rapidly resolidified layer of SG cast iron in the EDM process through the response surface methodology, J. Mater. Process. Technol. **182** (2007) 525–533

17. S.S. Habib, Study of the parameters in electrical discharge machining through response surface methodology approach, Appl. Math. Model. **33** (2009) 4397–4407
18. S. Prabhu, M. Uma, B.K. Vinayagam, Electrical discharge machining parameters optimization using response surface methodology and fuzzy logic modeling, J. Br. Soc. Mech. Sci. Eng. **36** (2013) 637–652
19. M. Hourmand, S. Farahany, A.A.D. Sarhan, M.Y. Noordin, Investigating the electrical discharge machining (EDM) parameter effects on Al-Mg2Si metal matrix composite (MMC) for high material removal rate (MRR) and less EWR–RSM approach, Int. J. Adv. Manufactur. Technol. **77** (2014) 831–838
20. R.V.H. Barenji, H. Pourasl, V.M. Khojastehnezhad, Electrical discharge machining of the AISI D6 tool steel: prediction and modeling of the material removal rate and tool wear ratio. Precis. Eng. **45** (2016) 435–444
21. A. Soundhar, H.A. Zubar, M.T.B.H. Sultan, J. Kandasamy, Dataset on optimization of EDM machining parameters by using central composite design, Data Brief **23** (2019) 103671
22. D. Mandal, S.K. Pal, P. Saha, Modeling of electrical discharge machining process using back propagation neural network and multi-objective optimization using non-dominating sorting genetic algorithm-II, J. Mater. Process. Technol. **186** (2007) 154–162
23. A.P.D. Markopoulos, E. Manolakos, N.M. Vaxevanidis, Artificial neural network models for the prediction of surface roughness in electrical discharge machining, J. Intell. Manufactur. **19** (2008) 283–292
24. M.K. Pradhan, R. Das, C.K. Biswas, Comparisons of neural network models on surface roughness in electrical discharge machining, Proc. Inst. Mech. Eng. B **223** (2009) 801–808
25. S.S. Sidhu, A. Batish, S. Kumar, Neural network-based modeling to predict residual stresses during electric discharge machining of Al/SiC metal matrix composites, Proc. Inst. Mech. Eng. B **227** (2013) 1679–1692
26. S. Kumar, A. Batish, R. Singh, T.P. Singh, A hybrid Taguchi-artificial neural network approach to predict surface roughness during electric discharge machining of titanium alloys, J. Mech. Sci. Technol. **28** (2014) 2831–2844
27. P. Ong, C.H. Chong, Bin M.Z.W. Rahim, K.C. Lee, K. Sia, M.A.H. Ahmad, Intelligent approach for process modelling and optimization on electrical discharge machining of polycrystalline diamond, J. Intell. Manufactur. (2018) doi:10.1007/s10845-018-1443-6
28. M. Lin, C. Tsao, C. Hsu, A. Chiou, P. Huang, Y. Lin, Optimization of micro milling electrical discharge machining of Inconel 718 by Grey-Taguchi method, Trans. Nonferrous Metals Soc. China **23** (2013) 661–666
29. A.M. Nikalje, A. Kumar, K.V.S. Srinadh, Influence of parameters and optimization of EDM performance measures on MDN 300 steel using Taguchi method, Int. J. Adv. Manufactur. Technol. **69** (2013) 41–49
30. L. Tang, Y.F. Guo, Electrical discharge precision machining parameters optimization investigation on S-03 special stainless steel, Int. J. Adv. Manufactur. Technol. **70** (2013) 1369–1376
31. V. Gaikwad, V.S. Jatti, Optimization of material removal rate during electrical discharge machining of cryo-treated NiTi alloys using Taguchi's method, J. King Saud Univ. **30** (2018) 266–272
32. J.H. Jung, W.T. Kwon, Optimization of EDM process for multiple performance characteristics using Taguchi method and Grey relational analysis, J. Mech. Sci. Technol. **24** (2010) 1083–1090
33. S. Singh, Optimization of machining characteristics in electric discharge machining of 6061Al/Al2O3p/20P composites by grey relational analysis, Int. J. Adv. Manufactur. Technol. **63** (2012) 1191–1202
34. U.S. Yadav, V. Yadava, Experimental modeling and multi-objective optimization of electrical discharge drilling of aerospace superalloy material, Proc. Inst. Mech. Eng. B **229** (2014) 1764–1780
35. R. Khanna, A. Kumar, M.P. Garg, A. Singh, N. Sharma, Multiple performance characteristics optimization for Al 7075 on electric discharge drilling by Taguchi grey relational theory, J. Ind. Eng. Int. **11** (2015) 459–472
36. L. Selvarajan, M. Manohar, U.A. Kumar, P. Dhinakaran, Modelling and experimental investigation of process parameters in EDM of Si3N4-TiN composites using GRA-RSM, J. Mech. Sci. Technol. **31** (2017) 111–122
37. C.-J. Tzeng, R.-Y. Chen, Optimization of electric discharge machining process using the response surface methodology and genetic algorithm approach, Int. J. Precis. Eng. Manufactur. **14** (2013) 709–717
38. S. Gopalakannan, T. Senthilvelan, Application of response surface method on machining of Al-SiC nano-composites, Measurement **46** (2013) 2705–2715
39. H.A.M. Hegab, H. Gadallah, A.K. Esawi, Modeling and optimization of Electrical Discharge Machining (EDM) using statistical design, Manufactur. Rev. **2** (2015) 21
40. R. Swiercz, D. Oniszczuk-S wiercz, T. Chmielewski, Multi-response optimization of electrical discharge machining using the desirability function, Micromachines **10** (2019) 72
41. Jagadish, A. Ray, Optimization of process parameters of green electrical discharge machining using principal component analysis (PCA), Int. J. Adv. Manufactur. Technol. **87** (2015) 1299–1311
42. S.N. Sahu, N.C. Nayak, Multi-criteria decision making with PCA in EDM of A2 tool steel. Mater. Today **5** (2018) 18641–18648
43. Y. Yildiz, M.M. Sundaram, K.P. Rajurkar, Statistical analysis and optimization study on the machinability of beryllium-copper alloy in electro discharge machining, Proc. Inst. Mech. Eng. B **226** (2012) 1847–1861
44. T. Muthuramalingam, B. Mohan, Influence of discharge current pulse on machinability in electrical discharge machining, Mater. Manufactur. Processes **28** (2013) 375–380
45. A. Torres, I. Puertas, C.J. Luis, EDM machinability and surface roughness analysis of INCONEL 600 using graphite electrodes, Int. J. Adv. Manufactur. Technol. **84** (2015) 2671–2688
46. Rahul, S. Datta, B.B. Biswal, S.S. Mahapatra, Machinability analysis of Inconel 601, 625, 718 and 825 during electro-discharge machining: on evaluation of optimal parameters setting, Measurement **137** (2019) 382–400
47. C.P.S. Mohanty, S. Mahapatra, J. Sahu, Parametric optimisation of electrical discharge machining process: a numerical approach, Int. J. Ind. Syst. Eng. **22** (2016) 207–244
48. J. Sahu, S.S. Mahapatra, C.P. Mohanty, Multi-response optimisation of EDM parameters using data envelopment analysis, Int. J. Product. Qual. Manag. **15** (2015) 309–334

49. C.P.S. Mohanty, S. Mahapatra, M.R. Singh, A particle swarm approach for multi-objective optimization of electrical discharge machining process, J. Intell. Manufactur. **27** (2014) 1171–1190
50. P. Mukhopadhyay, S. Adhikary, A.K. Samanta, S. Maiti, S. Khan, S. Mudi, External force assisted electro discharge machining of SS 316, Mater. Today **19** (2019) 626–629
51. N.R. Costa, J. Lourenço, Z.L. Pereira, Desirability function approach: a review and performance evaluation in adverse conditions, Chemometr. Intell. Lab. Syst. **107** (2011) 234–244
52. G. Skrabalak, Influence of electrode tool length on the micro EDM drilling performance, Proc. CIRP **68** (2018) 594–598

Cite this article as: Subhashree Naik, Sudhansu Ranjan Das, Debabrata Dhupal, Analysis, predictive modelling and multi-response optimization in electrical discharge machining of Al-22%SiC metal matrix composite for minimization of surface roughness and hole overcut, Manufacturing Rev. **7**, 20 (2020)